USAAMRDL-TR- 76-19

(12)

ANALYTICAL INVESTIGATION OF AN IMPROVED HELICOPTER LANDING GEAR CONCEPT

Hughes Helicopters
Division of The Summa Corporation
Culver City, Calif. 90230

August 1976

Final Report for Period June 1975 - February 1976

Prepared for

EUSTIS DIRECTORATE
U. S. ARMY AIR MOBILITY RESEARCH AND DEVELOPMENT LABORATORY
Fort Eustis, Va. 23604

EUSTIS DIRECTORATE POSITION STATEMENT

The feasibility of using a unique shock absorption and energy redistribution system for helicopter skid-type landing gears is analytically examined in this report. The findings indicate that such a system would greatly attenuate the landing loads experienced during hard and/or autorotational landings. The study also reavels that the incidence of main rotor blade/tail boom strikes is minimized and the resulting high velocity pitch and role modes are diminished. Ground resonance boundaries are shown to be increased approximately threefold.

William T. Alexander, Jr. of the Technology Applications Division served as project engineer for this effort.

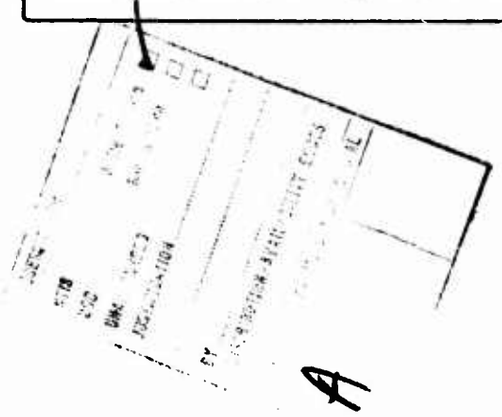

Unclassified

SECURITY CLASSIFICATION OF THIS PAGE (When Data Entered)

REPORT DOCUMENTATION PAGE	READ INSTRUCTIONS BEFORE COMPLETING FORM
1. REPORT NUMBER: USAAMRDL-TR-76-19	2. GOVT ACCESSION NO. / 3. RECIPIENT'S CATALOG NUMBER
4. TITLE (and Subtitle): ANALYTICAL INVESTIGATION OF AN IMPROVED HELICOPTER LANDING GEAR CONCEPT,	5. TYPE OF REPORT & PERIOD COVERED: Final Report, 30 Jun 75 – 19 Feb 76
	6. PERFORMING ORG. REPORT NUMBER: HH-76-37
7. AUTHOR(s): A. H. Logan	8. CONTRACT OR GRANT NUMBER(s): DAAJ02-75-C-0045
9. PERFORMING ORGANIZATION NAME AND ADDRESS: Hughes Helicopters, Division of Summa Corporation, Culver City, Cal. 90230	10. PROGRAM ELEMENT, PROJECT, TASK AREA & WORK UNIT NUMBERS: 62209A 1F262209AH76 00 080 EK
11. CONTROLLING OFFICE NAME AND ADDRESS: Eustis Directorate, U.S. Army Air Mobility Research and Development Laboratory, Fort Eustis, Va. 23604	12. REPORT DATE: Aug 76
	13. NUMBER OF PAGES: 84
14. MONITORING AGENCY NAME & ADDRESS (if different from Controlling Office): DA 1-T-262209 1-AH-76	15. SECURITY CLASS. (of this report): Unclassified
	15a. DECLASSIFICATION/DOWNGRADING SCHEDULE

16. DISTRIBUTION STATEMENT (of this Report)

Approved for public release; distribution unlimited

17. DISTRIBUTION STATEMENT (of the abstract entered in Block 20, if different from Report)

18. SUPPLEMENTARY NOTES

19. KEY WORDS (Continue on reverse side if necessary and identify by block number)

Landing Gear
Blade/Tailboom Interference
Helicopter

20. ABSTRACT (Continue on reverse side if necessary and identify by block number)

A design study has been conducted to define a landing gear concept that redistributes the impact energy of an autorotational landing in a manner that minimizes the occurrence of blade/tailboom strikes. The landing gear concept redistributes the impact energy by providing an interconnection between the front and rear landing gears. Through the interconnection, as the rear landing gear moves from the flight static position toward the full in position under landing impact, the front gear is impelled

OVER

DD FORM 1 JAN 73 1473 EDITION OF 1 NOV 65 IS OBSOLETE 4 04 152 Unclassified

SECURITY CLASSIFICATION OF THIS PAGE (When Data Entered)

20. Abstract - Continued

to move from the flight static position toward the full out position. When these motions have been accomplished, the skids (or front and rear wheels) are on the ground surface and the reactions inherent in absorbing the autorotational landing do not produce a pitching moment.

A physical design was developed for the OH-6A and compared to the landing gear provisions of MIL-STD-1290. Ground resonance, weight, and life cycle cost analyses were also performed.

The analysis indicates that pitch interconnection significantly reduces the nose-down pitching moment that occurs during nose-high autorotation. This increases blade/tailboom spacing, which eliminates the majority of blade/tailboom strikes.

Roll interconnection increases the ground resonance boundaries threefold.

SUMMARY

A preliminary design study has been conducted to define a landing gear concept that redistributes the impact energy of an autorotational landing in a manner that minimizes the occurrence of blade/tailboom strikes. The resulting landing gear concept redistributes the impact energy and reduces the nose-down pitching moment by providing an interconnection between the front and rear landing gears. Through the interconnection, as the rear landing gear moves from the flight static position toward the full in position under landing impact, the front gear is impelled to move from the flight static position toward the full out position. When these motions have been accomplished, the skids (or front and rear wheels) are on the ground surface and the vertical reactions inherent in absorbing the autorotational landing do not produce a pitching moment.

During the initial phase of the preliminary design, an analytical model was used to define the dynamic characteristics of the interconnected landing gear. Based on these dynamic characteristics, a suggested physical design was developed for the OH-6A. This proposed design was then examined for energy absorption capabilities as compared to the landing gear provisions of MIL-STD-1290. Ground resonance, weight, and life-cycle cost analyses were also performed as inputs to a penalties versus performance gains analysis.

The analysis indicates that pitch interconnection significantly reduces the nose-down pitching moment that occurs during nose-high autorotation. This increases blade/tailboom spacing, which eliminates the majority of blade/tailboom strikes. Life-cycle cost analysis of the interconnected landing gear indicates that the reduction in helicopter damage results in savings of more than twice the original modification cost.

When the landing gear is interconnected in the roll mode, the ground resonance boundaries are increased threefold.

The interconnected landing gear designed for the OH-6A requires only minor modification to the basic OH-6A landing gear. The cross tube is lengthened 8.32 inches and the damper/cross tube attachment has been modified to provide the increased travel required for interconnection.

PREFACE

This report was prepared by Hughes Helicopters, Division of Summa Corporation, under Contract No. DAAJ02-75-C-0045, funded by the U.S. Army Air Mobility Research and Development Laboratory (Eustis Directorate), Fort Eustis, Virginia. It covers the work performed during the period July 1975 to March 1976 and is the final technical report summarizing the activity. The USAAMRDL technical monitor for this contract was William Alexander. The Hughes Helicopter project manager was A. H. Logan, who also prepared the final report.

The author wishes to acknowledge R. A. Wagner, Manager, Research and Development Department, for his overall guidance and consultation in the preparation of this report. The author also wishes to acknowledge the following Hughes personnel: S.V. LaForge, who developed the computational analysis; H. M. Childers, who performed the ground resonance analysis; R.V. March, for the weights estimate; A. Neugebauer, for the life-cycle costs; and J. F. Needham, for the stress analysis.

TABLE OF CONTENTS

TABLE OF CONTENTS (CONT)

LIST OF ILLUSTRATIONS

LIST OF ILLUSTRATIONS (CONT)

LIST OF ILLUSTRATIONS (CONT)

LIST OF TABLES

INTRODUCTION

Blade/tailboom strikes occur with an excessive frequency during emergency autorotations. Many of these strikes have resulted in substantial damage to the helicopter and in fatalities and injuries to personnel. In addition, current Army size limitations require more compact helicopter designs which bring the tailboom and main rotor closer together, increasing the possibility of blade-boom contact.

The sequence of events which results in blade/tailboom strikes in emergency (or practice) autorotations many times follows this pattern:

1. Ground contact is made with the helicopter in a nose-up attitude.

2. The vertical reaction loads act to give a nose-down moment on the helicopter. This nose-down moment is increased due to drag loads if forward speed is present at contact.

3. This nose-down moment causes angular acceleration and nose-down angular velocity (nose-down angular velocity is also tailboom-up angular velocity).

4. Pilot reaction to nose-down velocity is to pull the cyclic stick back. This tends to bring the rotor blades down in the rear while the boom is coming up. This combination aggravates main rotor blade and tailboom interference.

It should be evident that whatever reduces the nose-down pitching moment will reduce the tendency toward boom chops. This fact is widely recognized, and pilots are trained to level the helicopter prior to ground contact for the sole reason of reducing the nose-down moment.

Unfortunately, this maneuver requires considerable judgment and finesse in handling both the cyclic and collective controls. Additionally, the act of leveling the helicopter prior to touchdown reduces the angle of attack of the rotor, and hence, reduces the lift on the rotor at the wrong time in the maneuver.

What is required is a landing gear that redistributes the impact energy of an autorotational landing in a manner that minimizes the occurrence of blade/tailboom strikes and reduces the pilot workload. Previous studies have defined specific landing gear changes that do reduce the

nose-down pitching moment and reduce blade/tailboom strikes.[1,2] However, these changes apply to a specific landing gear and are not readily transferable to other landing gear designs. The intent of this study, therefore, was to develop a successful design that demonstrates principles applicable to any landing gear configuration.

A preliminary design study has been conducted to define a landing gear concept which reduces the nose-down pitching moment by providing an interconnection between the front and rear landing gears. Through the interconnection, as the rear landing gear moves from the flight static position toward the full in position under landing impact, the front gear is impelled to move from the flight static position toward the full out position. When these motions have been accomplished, the skids (or front and rear wheels) are on the ground surface, and the vertical reactions inherent in absorbing the autorotational landing do not produce a pitching moment.

For purposes of preliminary design, the OH-6A was used as the baseline aircraft, and the interconnected landing gear was designed to require minimum modification to the OH-6A. Consequently, the interconnected landing gear is a skid type gear, as used on the OH-6A. However, the basic design principles also apply to wheel type landing gear. The difference is that, in wheel type gear, the interconnected front and rear supports are attached to independent wheels and not a skid tube common to all supports.

During the initial phase of the preliminary design, an analytical model was used to define the dynamic characteristics of the interconnected landing gear. Based on these dynamic characteristics, a suggested physical design was developed. This proposed design was then examined for energy absorption capabilities as compared to the landing gear provisions of MIL-STD-1290. Ground resonance, weight, and life-cycle cost analyses were also performed as inputs to a penalties versus performance gains analysis.

---

[1] Currier, E.J., et al, PRELIMINARY DESIGN AND ANALYSIS REPORT, REDUCTION OF VULNERABILITY TO TAILBOOM/BLADE STRIKES, Hughes Tool Company - Aircraft Division Report 369-V-3603, October 1970.

[2] Amer, K.B., PROPOSED OH-6A PRODUCT IMPROVEMENT PROGRAM TO IMPROVE AUTOROTATION LANDING CHARACTERISTICS, Hughes Tool Company - Aircraft Division Report 369-V-3603P, January 1970.

INTERCONNECTED LANDING GEAR DESIGN

A preliminary design for an interconnected landing gear was developed within four main constraints: The interconnected landing gear is to be designed for the OH-6A; the OH-6A will require minimum modification to accommodate the interconnected landing gear; the interconnected gear must satisfy the MIL-STD-1290 requirement of not penetrating either occupiable areas or flammable fluid containers during a crash; and the OH-6A exterior physical envelope must be maintained. For the landing gear design, the important physical envelope to be maintained is the maximum nose-up angle before the tail skid touches the ground.

The present OH-6A landing gear arrangement is a skid type and is shown diagrammatically in Figure 1. The skid is attached to front and rear angled cross tubes which are each attached to the fuselage at a single pivot point. Dampers are attached at the elbow of each cross tube and then fixed to the fuselage. Landing energy is absorbed in the linear compression of the oleo dampers, which allows the cross tubes to rotate in a vertical plane about their pivot points. Maximum landing energy is absorbed by cross tube yielding. With this basic design in mind, the modifications required to design an interconnected landing gear system are considered.

Pitch Interconnection

The pitch interconnected landing gear for the OH-6A is essentially the basic landing gear with three modifications as shown in Figure 2. The oleo damper/cross tube attachment has been modified to provide additional vertical movement required by pitch interconnection; the cross tube has been lengthened 8.32 inches at the cross tube/skid attachment; and the front and rear dampers have been connected through a low constraint interconnect. The basic fuselage pivot points, drag braces, and skids remain unchanged. By treating only the oleo dampers, the required modifications to the OH-6A are minimized. As will be shown, the only modifications required are an enlargement of the landing gear opening in the skin to accommodate the additional travel and the relocation of the oleo damper upper attachment points. The extended length cross tube is constructed in the same manner as the present extended cross tube for the commercial Hughes 500C (part number 369H-6001), which extends the landing gear 18 inches. In this construction, the basic cross tube is approximately the same length as the present OH-6A. However, the cross tube/skid juncture is now open to allow an insert between the skid

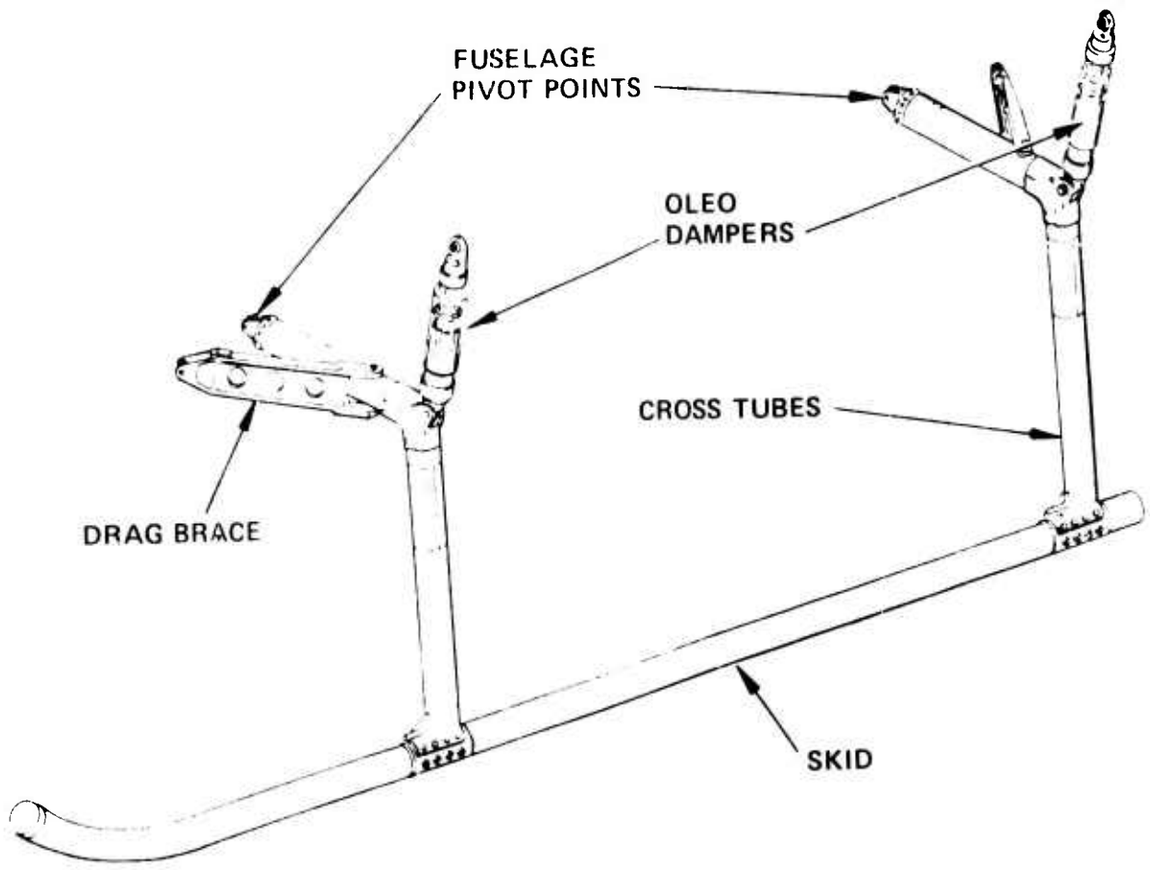

Figure 1. Diagram of Current OH-6A Landing Gear

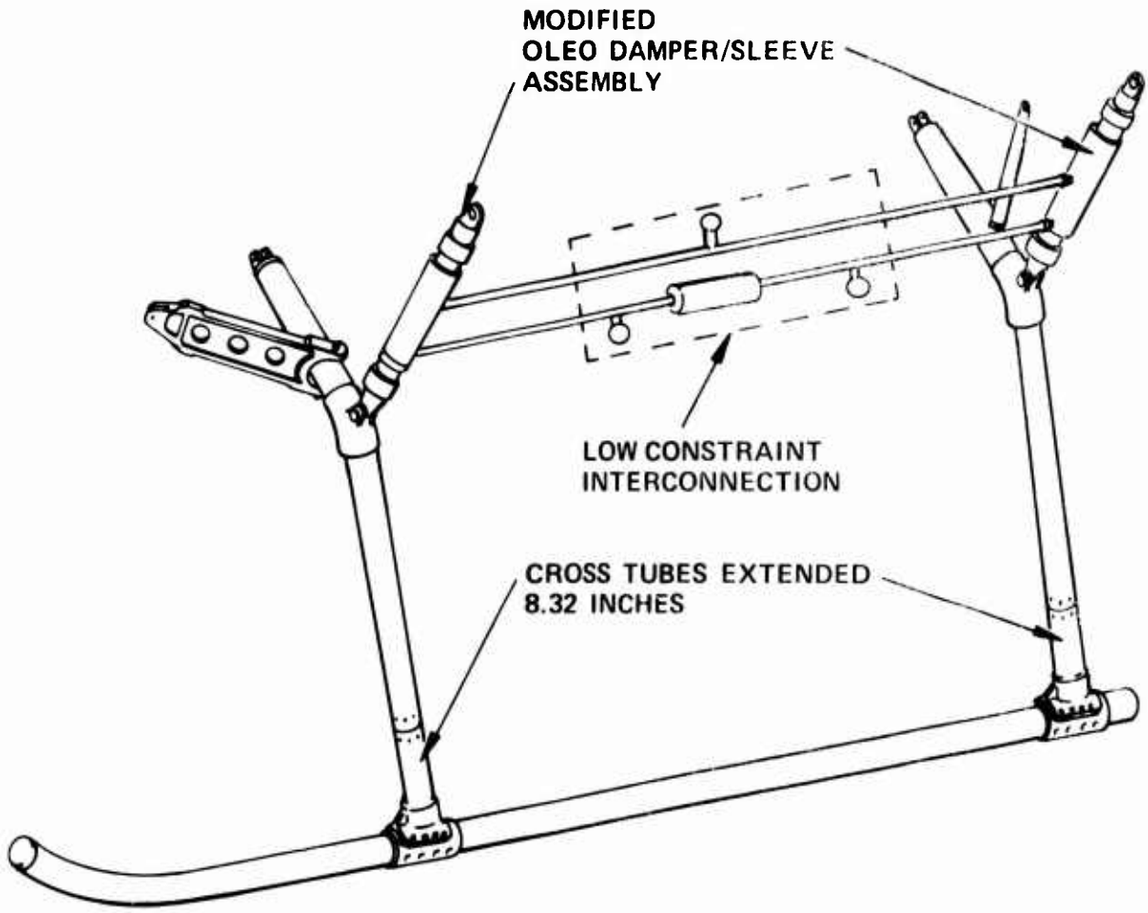

Figure 2. Diagram of Pitch Interconnected Landing Gear for the OH-6A

and the cross tube. In addition to increasing the length, the commercial Hughes 500C cross tube has a higher yield strength than the basic OH-6A cross tube.

For the damper/cross tube attachment modification, the basic front and rear oleo dampers (369H92131) now fit into new sleeves which are attached to the cross tubes (Figure 3). Each sleeve provides an additional 1.74 inches of travel both up and down from the neutral position. For each sleeve, two annular chambers filled with hydraulic fluid are formed by sealing the sleeve to the basic oleo damper. Matching hydraulic chambers on the front and rear dampers are connected through a low constraint interconnection system as shown in Figure 4. During a nose-high auto-rotational landing, when the aft skid experiences high force and the forward

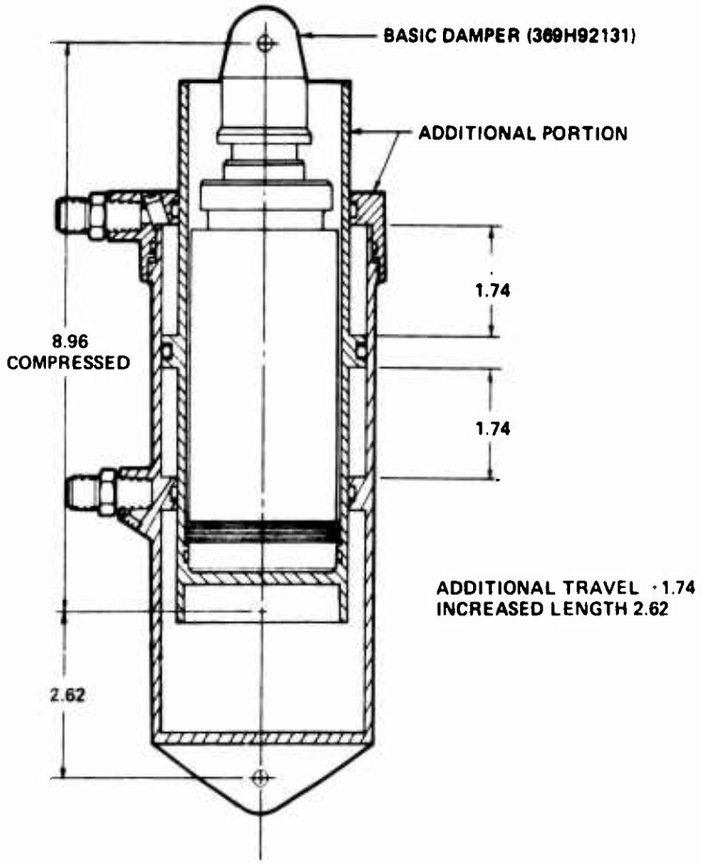

Figure 3. Modified Oleo Damper/Sleeve Assembly for Interconnected Landing Gear

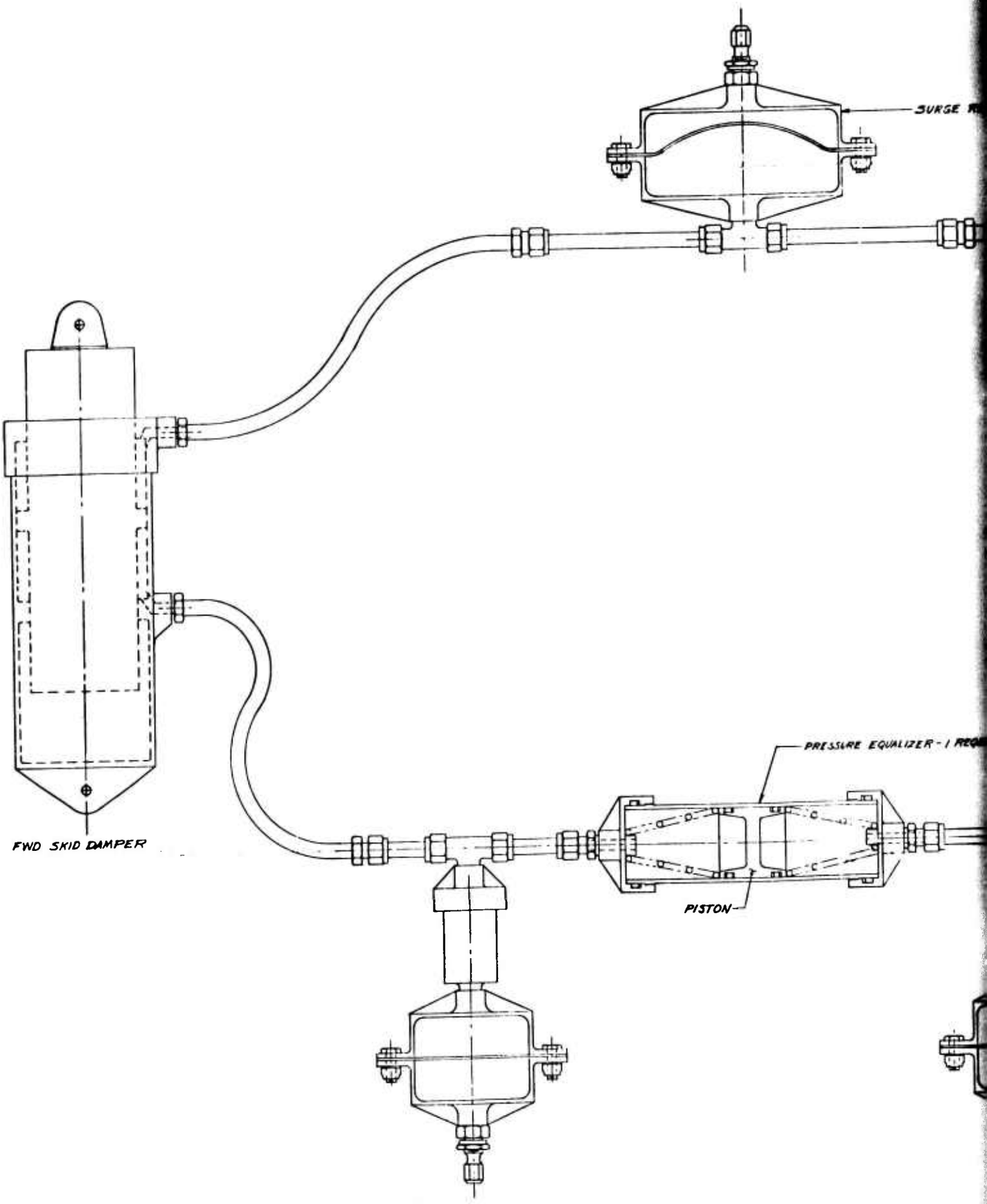

Figure 4. Schematic of Interconnected Landing Gear Actuator

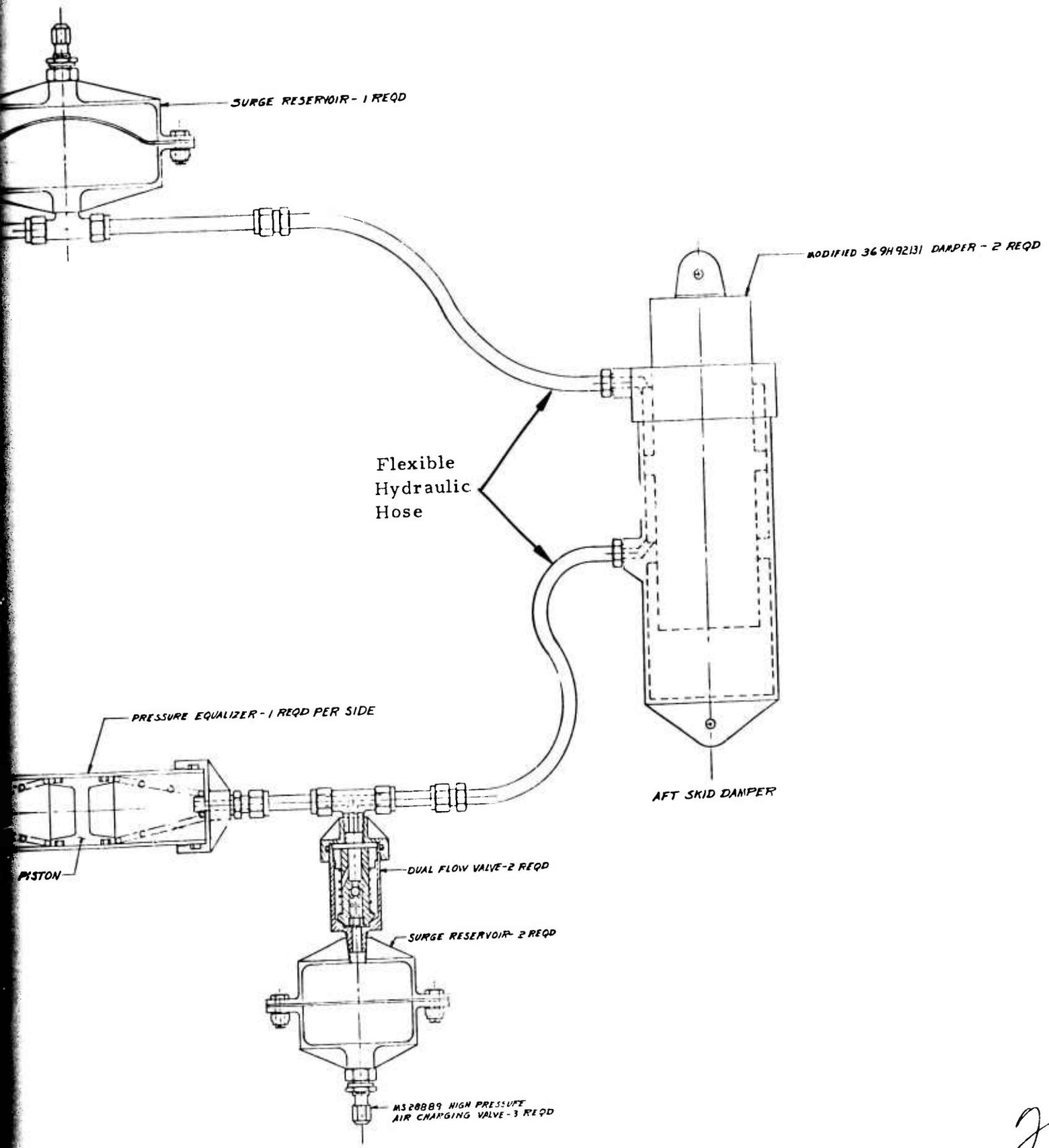
SURGE RESERVOIR - 1 REQD
MODIFIED 369H92131 DAMPER - 2 REQD
Flexible
Hydraulic
Hose
PRESSURE EQUALIZER - 1 REQD PER SIDE
AFT SKID DAMPER
PISTON
DUAL FLOW VALVE - 2 REQD
SURGE RESERVOIR - 2 REQD
MS28889 HIGH PRESSURE
AIR CHARGING VALVE - 3 REQD

2

skid little force, the aft skid damper is compressed, forcing hydraulic fluid out of the lower aft chamber, into the pressure equalizer. This creates unequal pressure in the pressure equalizer, moving the piston forward, forcing hydraulic fluid into the lower forward chamber. This causes the forward skid damper to extend down while the aft skid damper compresses upward.

As shown in Figure 4, the low constraint interconnection system is comprised of a pressure equalizer (or spring/damper system) and three surge reservoirs. The pressure equalizer senses differential hydraulic pressure between the forward and aft oleo dampers and moves a spring assembly to accommodate the differential force. This operates primarily during nose-high (or nose-low) autorotational landings when the aft skid senses the landing force and the forward skid is off the ground, sensing little or no force. The two lower surge reservoirs act when there is a level landing and the front and rear skid dampers experience similar forces. Then, the line pressures are nearly equal and build to high levels. Once a certain level of line pressure is reached, the dual flow valves on the lower surge reservoirs open and allow the line hydraulic fluid to fill the reservoirs. This acts as a pressure relief valve to limit line pressures to allow the use of low pressure tubing. The upper surge reservoir is used at all times to provide fluid to the system and to prevent cavitation.

Based on analytical studies, the pressure equalizer acts as a spring with a spring constant of 103 lb/in. and a damping at $10.3 \frac{\text{lb}}{\text{in./sec}}$. The lower surge reservoirs act only above line pressures of 100 psi.

The cross tube length was extended so that the angle from the present OH-6A landing gear skid to the tail skid for autorotation landings would be maintained for the basic OH-6A and for the interconnection system once the interconnected movement was accounted for (see Figure 5). This feature becomes important because the interconnection system reduces nose-down (tail up) pitching movement, causing the tail skid-ground clearance to be less than the basic OH-6A. Lengthening the cross tube maintains this clearance.

The range of skid movements for the interconnected system is shown in Figure 6. The skid has a pitch range of approximately 10 degrees about its neutral position, giving a resultant angle of 13 degrees 40 minutes due to the approximate 3-degree downward tilt already built into the landing gear. As is shown in Figure 6, the additional travel required the hole in the skin to be elongated.

The 10 degrees of skid interconnection movement was determined by the additional damper linear travel that was available without major modification to the OH-6A. Another factor influencing the determination of 10 degrees of skid interconnection movement was the fact that both front and rear modified oleo damper/sleeve assemblies are the same. Consequently, the limit on additional damper travel found for either the front or rear modified damper assembly also applied to the other assembly, rear or front, respectively. This coupling of damper travel limits was the result of the effort to minimize the number of new parts needed for the interconnection system by making the front and rear modified oleo damper/sleeve assemblies the same.

The additional damper linear travel available was determined by the pilot seat location. Since the cross tubes remain in the same position between the basic OH-6A and the interconnected system, the additional travel required by the interconnected damper/sleeve assembly could only come from moving the upper attachment point. This was limited in the front by the pilot seats. Any further extension would infringe on the pilot area, requiring major modification to the aircraft. Since the front and rear modified assemblies are the same, the limit imposed by the pilot's seat on the front damper/sleeve also limited the rear assembly. The relocation of the upper oleo attachment point and the elongation of the skin hole for both the front and rear landing gear are the only modifications to the basic OH-6A.

The hydraulic interconnection system satisfies the major design constraints. The interconnection system fits into the present OH-6A, requiring only minor modifications. With no rigid connections between the front and rear cross tubes, there is no chance of penetrating either occupiable areas or flammable fluid containers during a crash. Accordingly, the design concept derived herein incorporates the application of flexible high-pressure hydraulic hose and breakaway connections. Rigid interconnection systems were examined during preliminary design but were discarded because they did not meet this MIL-STD-1290 requirement.

Roll Interconnection

The roll interconnection of the landing gear is accomplished in a manner similar to the pitch interconnection shown in Figure 2. The additional number of parts required are fewer than for pitch. For roll interconnection, two additional pressure equalizers are needed; one interconnecting the front modified damper/sleeve assemblies and one between the rear

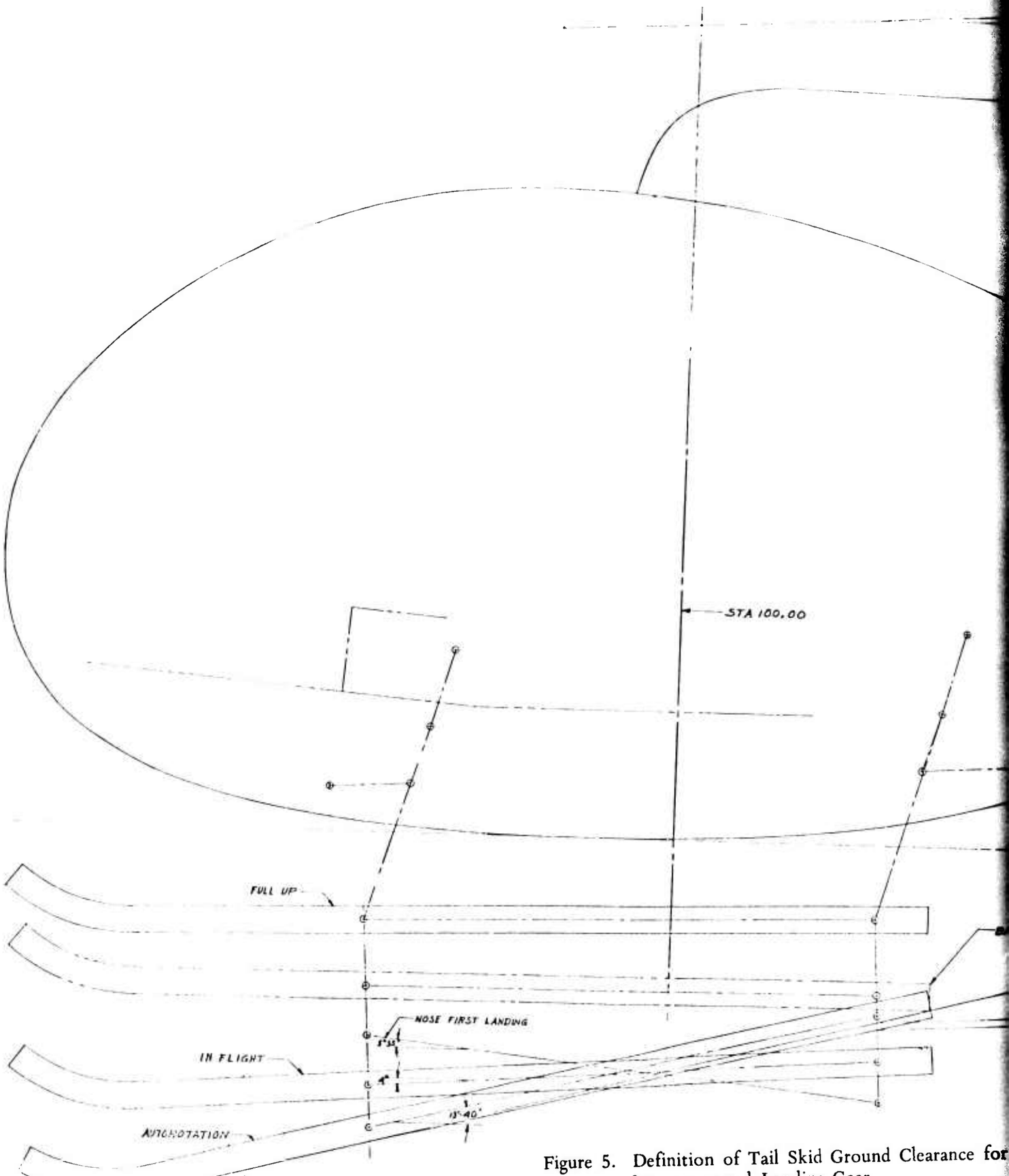

Figure 5. Definition of Tail Skid Ground Clearance for Interconnected Landing Gear

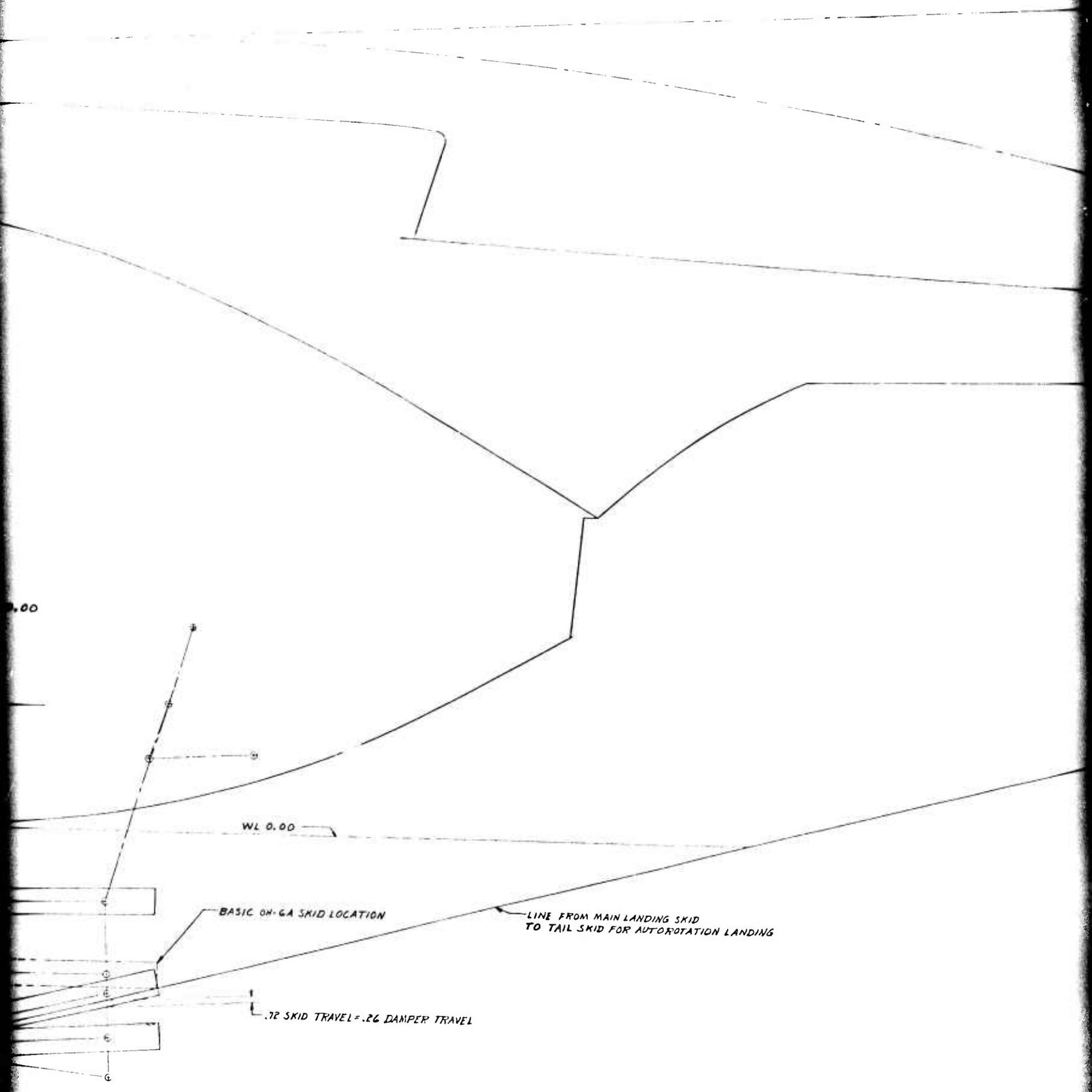

Skid Ground Clearance for
nding Gear

2

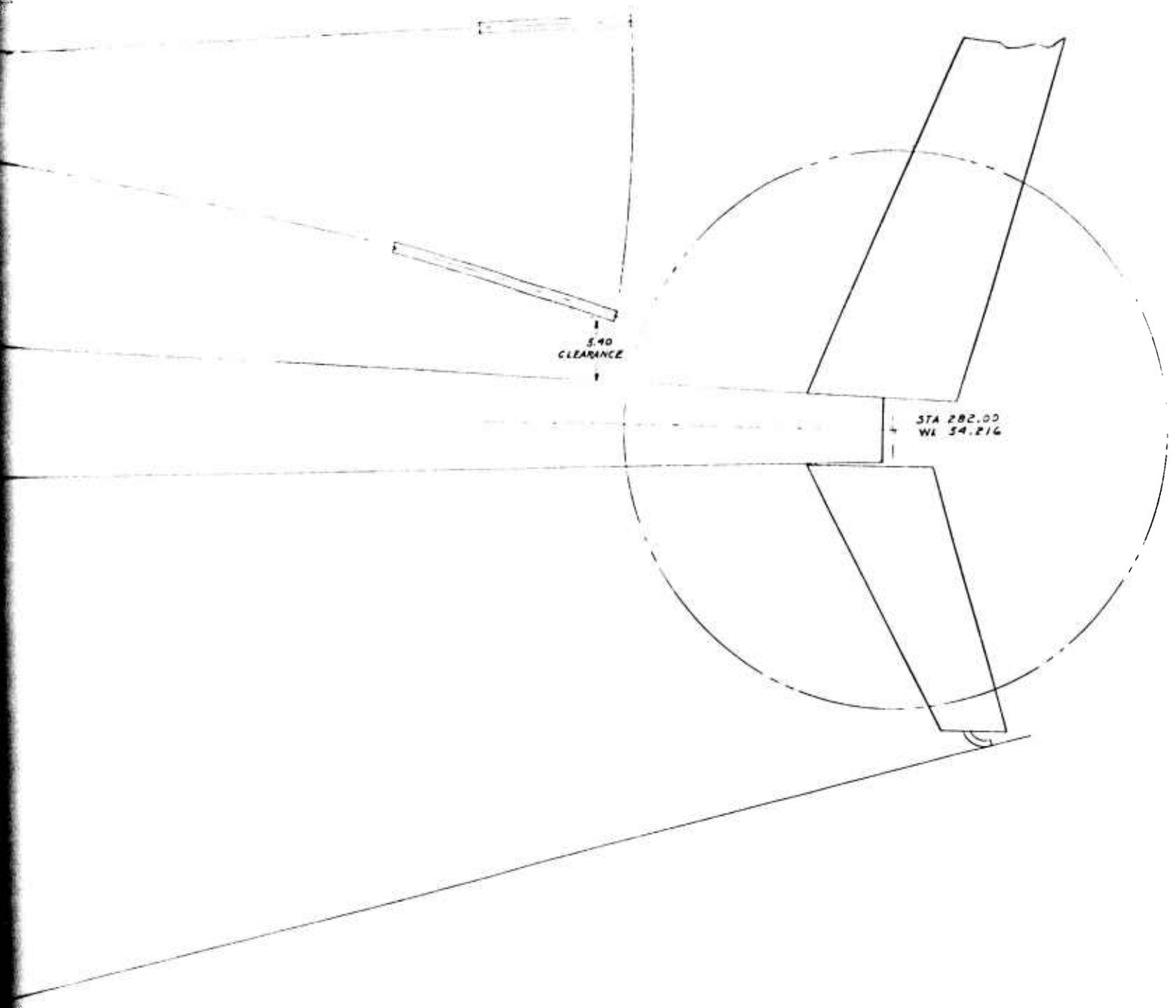
5.90
CLEARANCE
STA 282.00
WL 54.216

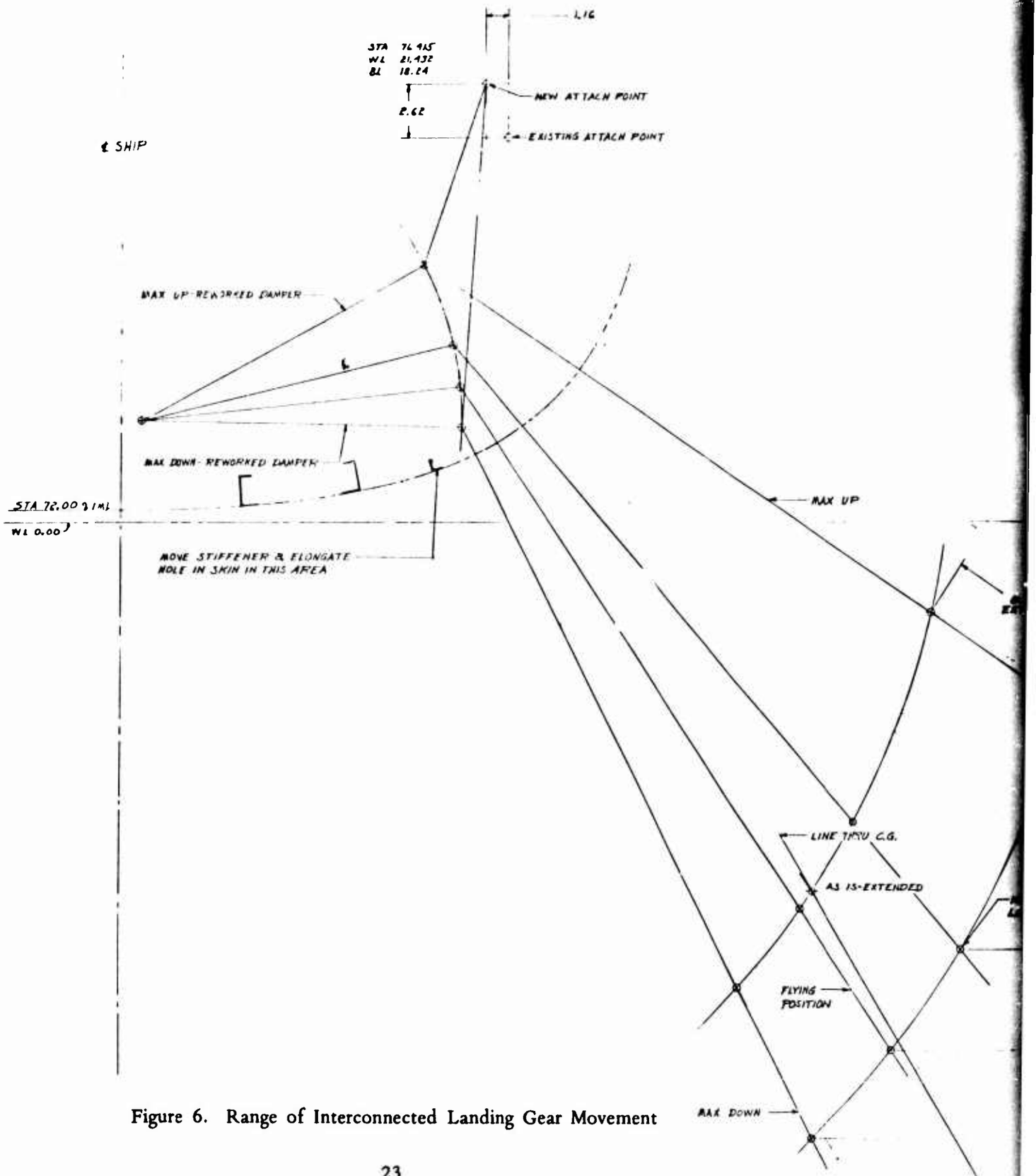

Figure 6. Range of Interconnected Landing Gear Movement

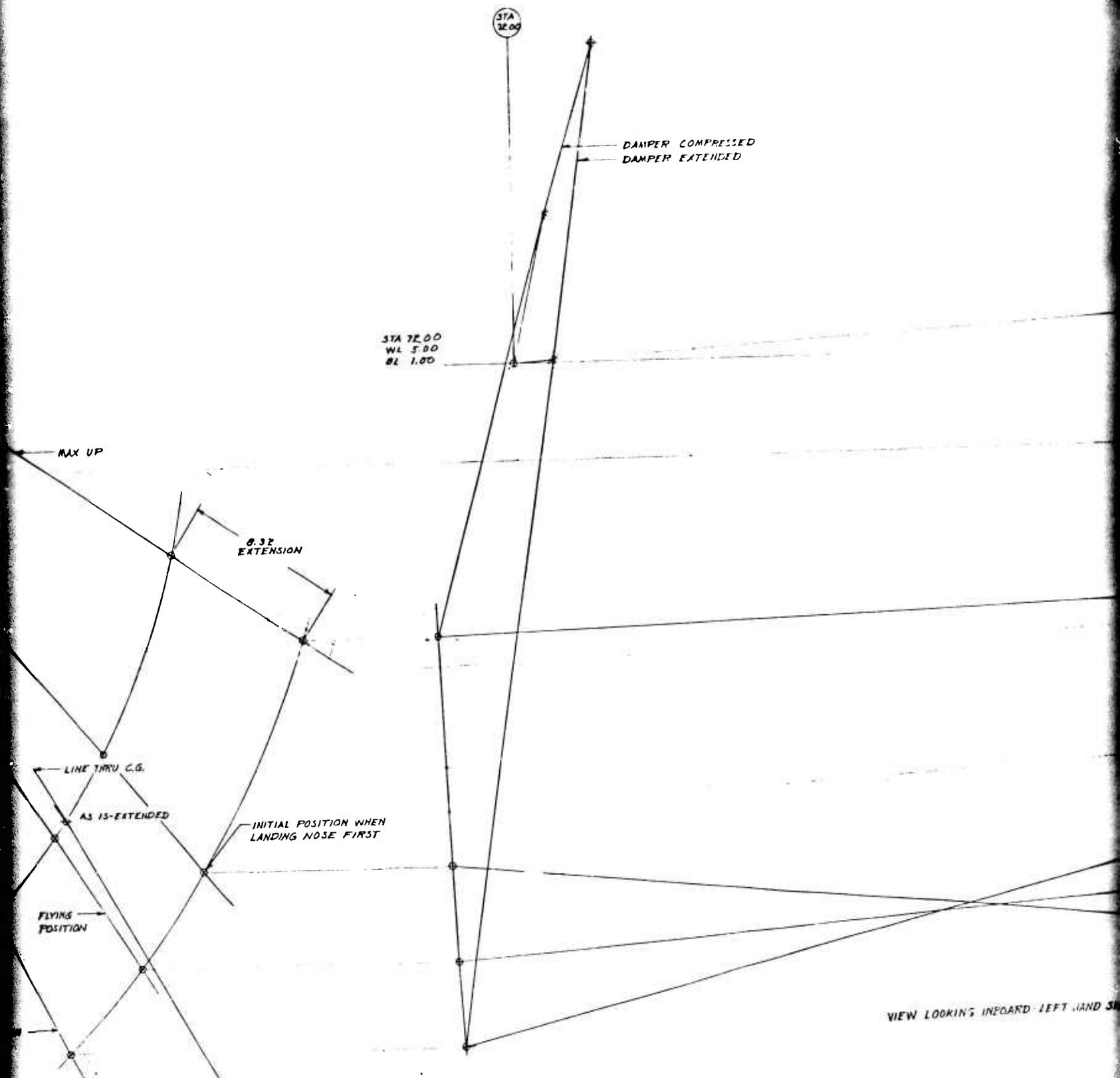
STA 72.00
DAMPER COMPRESSED
DAMPER EXTENDED
STA 72.00
WL 5.00
BL 1.00
MAX UP
8.32 EXTENSION
LINE THRU C.G.
AS IS-EXTENDED
INITIAL POSITION WHEN LANDING NOSE FIRST
FLYING POSITION
VIEW LOOKING INBOARD - LEFT HAND

2

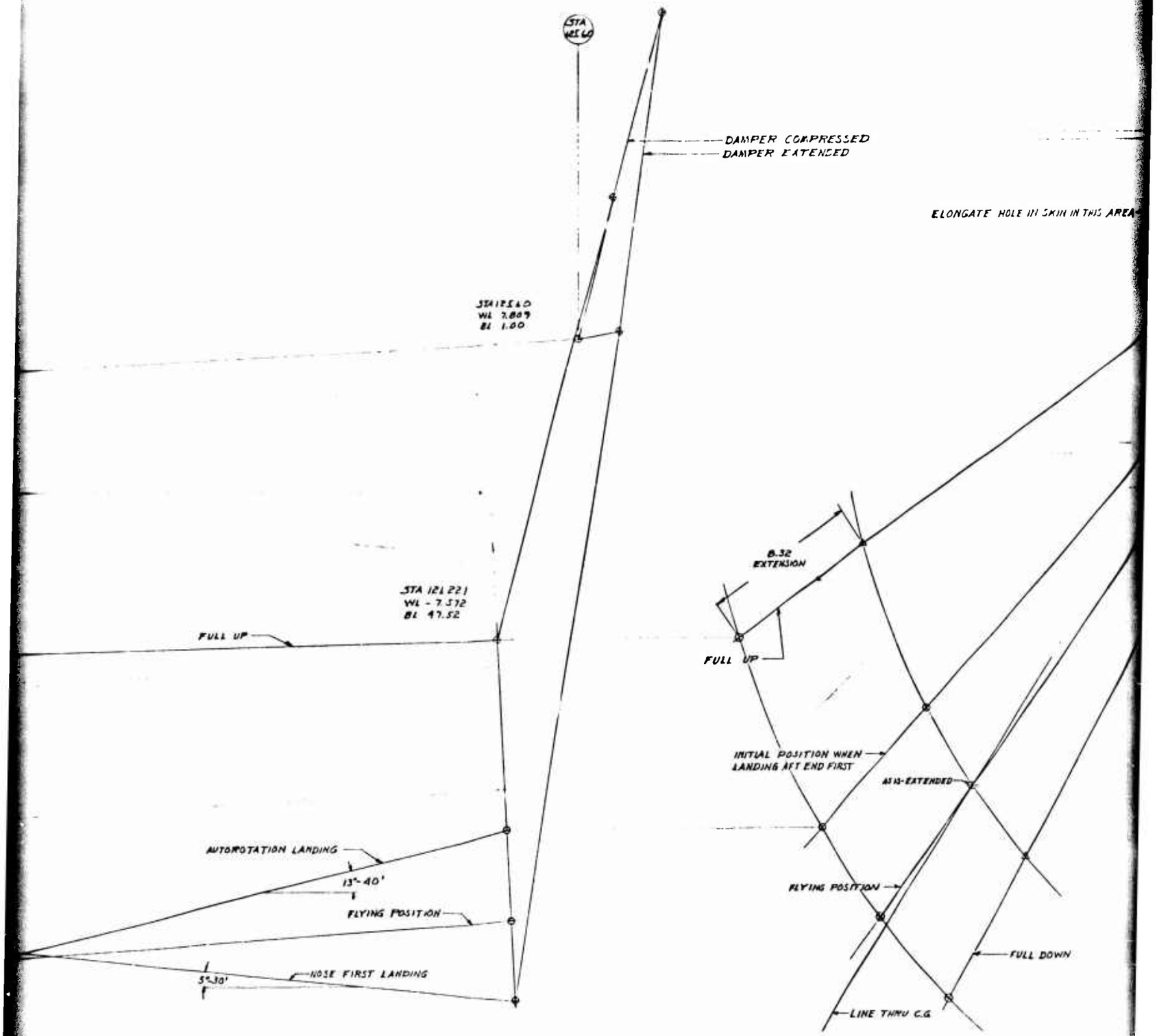

INBOARD - LEFT HAND SIDE

3

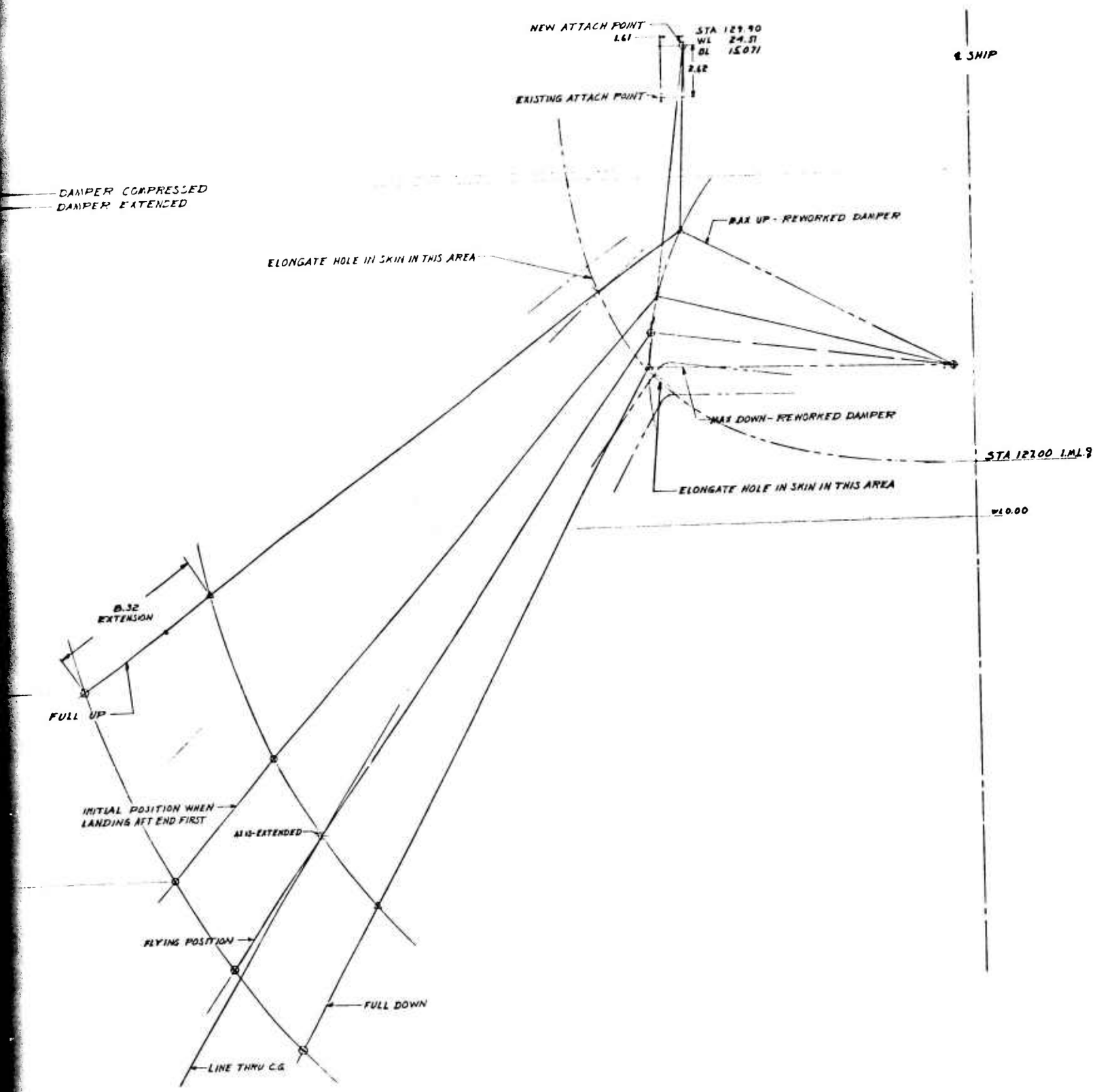
NEW ATTACH POINT
1.61
STA 129.90
WL 24.51
BL 15.071
2.62
EXISTING ATTACH POINT
℄ SHIP
DAMPER COMPRESSED
DAMPER EXTENDED
MAX UP - REWORKED DAMPER
ELONGATE HOLE IN SKIN IN THIS AREA
MAX DOWN - REWORKED DAMPER
STA 122.00 I.ML.S
ELONGATE HOLE IN SKIN IN THIS AREA
WL 0.00
8.32
EXTENSION
FULL UP
INITIAL POSITION WHEN
LANDING AFT END FIRST
AXIS-EXTENDED
FLYING POSITION
FULL DOWN
LINE THRU C.G.

damper/sleeve assemblies. The three surge reservoirs in the pitch interconnection perform the same function in roll interconnection, eliminating the need for duplicate components in roll.

The pressure equalizer used in roll interconnection is the same as the equalizer used in pitch. A new equalizer was not developed specifically for roll because it was found that the equalizer optimized for pitch gave satisfactory performance in roll and the number of new parts required for the interconnected landing gear is minimized, reducing costs.

Stress Analysis

The proposed design of a pitch and roll interconnected landing gear for the OH-6A contains two features that impact heavily on the structural integrity of the helicopter. These are the longer cross tube and the increased yield strength of the cross tube. As will be shown later, these two features allow the interconnected landing gear to accept higher downward drop velocities than the basic OH-6A which translates into larger loads at the fuselage/landing gear attachment points. Specifically, the critical stress locations become the oleo upper attachment point to the fuselage and the attachments of the drag brace and inboard end of the cross tube to the keel beam of the OH-6A.

The level of the oleo damper load is a strong indicator of the severity of the loads in the landing gear and its supporting fuselage structure. A typical OH-6A experimental load distribution in the drag brace and cross tube attachment points is shown in Figure 7 for a reserve energy drop velocity of 8.17 feet per second. Experimental data at higher drop velocities indicate that the ratios of drag brace and cross tube attachment loads to the local oleo load (fore or aft) changes little over a wide range of drop velocities. Relations such as shown in Figure 7 have been used to design both the original OH-6A landing gear supporting structure and the subsequent improvements. Consequently, fuselage structure which is capable of reacting the ultimate oleo load would be capable of reacting the drag brace and cross tube loads.

The landing gear computer analysis predicts that the maximum rear and front oleo loads will be approximately 5900 pounds and 7000 pounds, respectively, for the interconnected landing gear at 2550 pounds gross weight and a vertical drop velocity of 19.5 feet per second, as shown in Figure 8. These are ultimate loads on the fuselage structure because gear contact velocities above 19.5 feet per second cause the cross tube to yield, making the cross tube incapable of transmitting any higher loads to the fuselage. The additional landing impact energy associated with

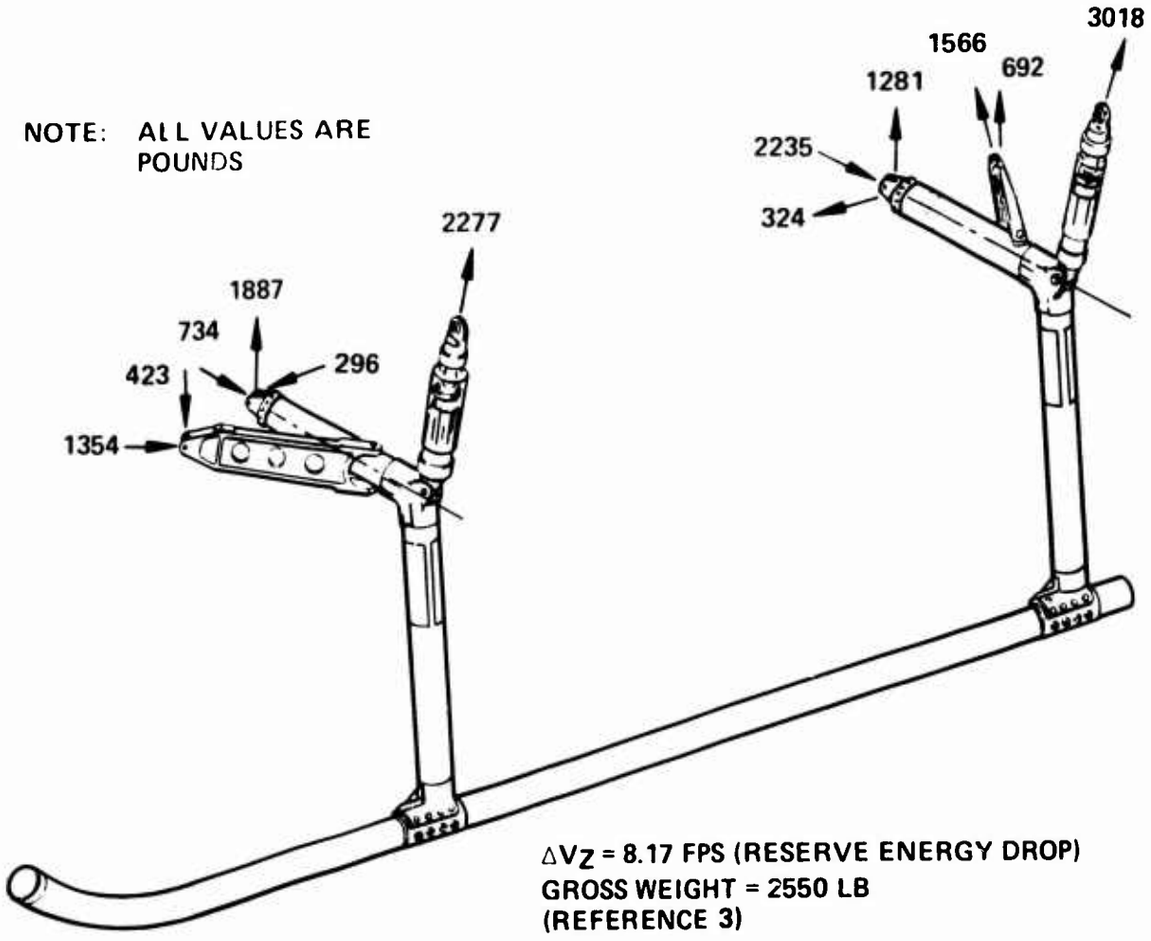

Figure 7. Typical OH-6A Experimental Load Distribution in Landing Gear Fuselage Supporting Structure

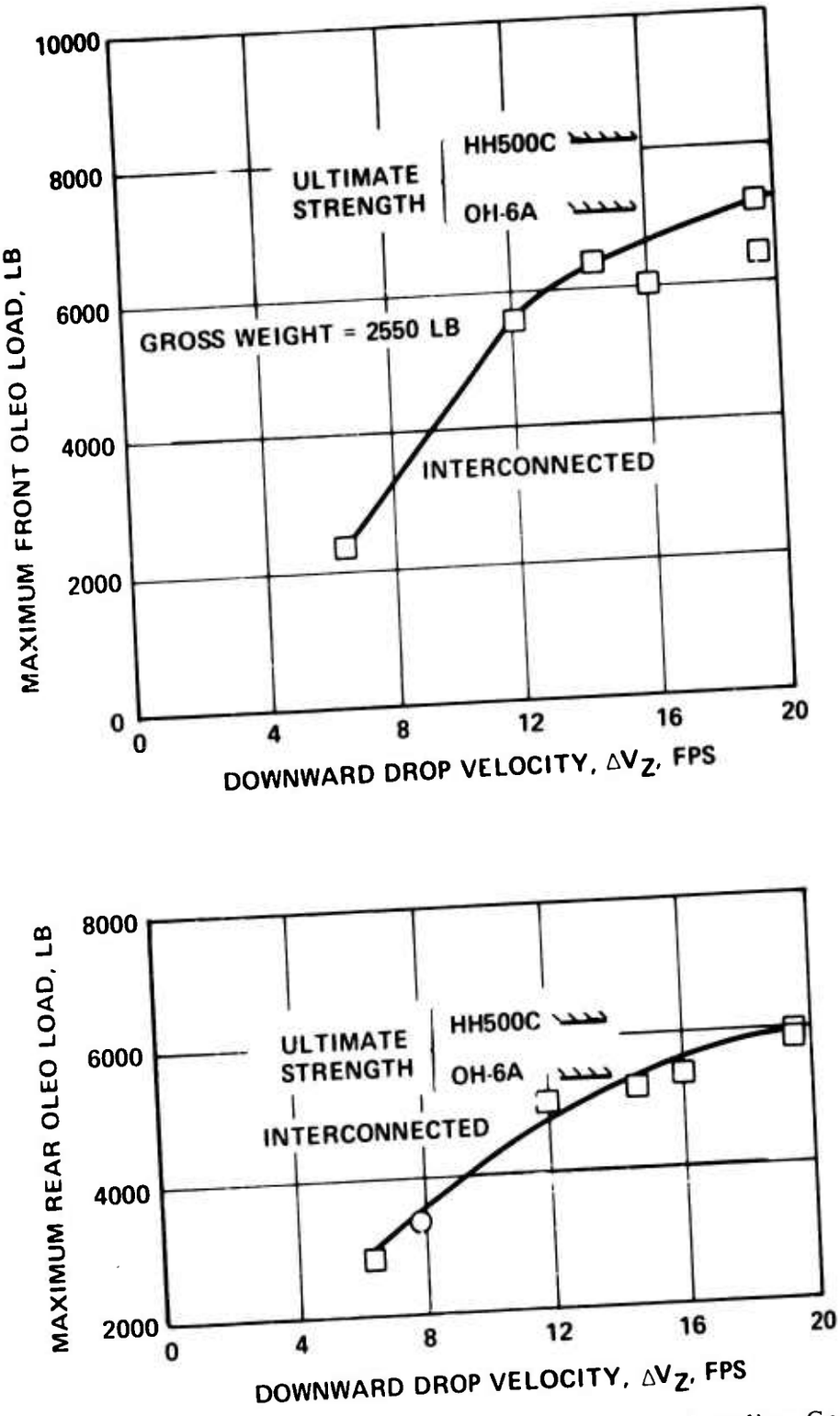

Figure 8. Variation of Predicted Interconnected Landing Gear Maximum Oleo Loads With Downward Drop Velocity

contact velocities above 19.5 feet per second is absorbed primarily by fuselage crushing. These loads are considered to be conservative because the predicted oleo loads tend to be higher than measured during actual drop tests. This is shown in Figure 9 for the basic OH-6A over a range of drop velocities and drop attitudes (nose up and level).

The present OH-6A is designed for a 5100-pound ultimate load in the rear oleo and 6750 pounds in the front oleo. These values reflect a minimum ultimate margin of safety of 6 percent. The calculated strength for the rear oleo support structure is 5400 pounds and for the forward structure is 7200 pounds. A comparison of these ultimate strengths and the interconnected landing gear maximum predicted oleo loads indicates that the OH-6A fuselage structure could be strengthened with only minor modification. When the OH-6A was translated into the commercial Hughes 500C, the fuselage landing gear support structure was increased in strength by approximately 15 percent. This resulted in the rear oleo support structure strength being 6200 pounds and the forward strength being 8200 pounds. In light of the conservative nature of the predicted loads, these increased values appear sufficient to sustain the maximum interconnected loads, as shown in Figure 8.

The upper damper/fuselage attachment points have to be moved to accommodate the interconnected landing gear travel, and the increased strength features of the 500C may be incorporated. Similarly, minor modifications may be made for the keel/drag brace attachment. (The HH 500C landing gear support structure modifications are found in drawing 369ASK1114.)

Weight

A detailed weight estimate indicates that the pitch interconnected landing gear system would add 40.9 pounds to the OH-6A's current weight. For roll interconnections, an additional 6.2 pounds is added to the OH-6A, bringing the total additional weight to 47.1 pounds for both pitch and roll interconnections. A listing of the individual weights of the pitch interconnection components is shown in Table 1. As listed, the largest weight increases are due to the modified dampers and the pressure equalizer. The additional weight for the roll interconnection is relatively low since the modified dampers would already have been added for pitch interconnection.

contact velocities above 19.5 feet per second is absorbed primarily by fuselage crushing. These loads are considered to be conservative because the predicted oleo loads tend to be higher than measured during actual drop tests. This is shown in Figure 9 for the basic OH-6A over a range of drop velocities and drop attitudes (nose up and level).

The present OH-6A is designed for a 5100-pound ultimate load in the rear oleo and 6750 pounds in the front oleo. These values reflect a minimum ultimate margin of safety of 6 percent. The calculated strength for the rear oleo support structure is 5400 pounds and for the forward structure is 7200 pounds. A comparison of these ultimate strengths and the interconnected landing gear maximum predicted oleo loads indicates that the OH-6A fuselage structure could be strengthened with only minor modification. When the OH-6A was translated into the commercial Hughes 500C, the fuselage landing gear support structure was increased in strength by approximately 15 percent. This resulted in the rear oleo support structure strength being 6200 pounds and the forward strength being 8200 pounds. In light of the conservative nature of the predicted loads, these increased values appear sufficient to sustain the maximum interconnected loads, as shown in Figure 8.

The upper damper/fuselage attachment points have to be moved to accommodate the interconnected landing gear travel, and the increased strength features of the 500C may be incorporated. Similarly, minor modifications may be made for the keel/drag brace attachment. (The HH 500C landing gear support structure modifications are found in drawing 369ASK1114.)

Weight

A detailed weight estimate indicates that the pitch interconnected landing gear system would add 40.9 pounds to the OH-6A's current weight. For roll interconnections, an additional 6.2 pounds is added to the OH-6A, bringing the total additional weight to 47.1 pounds for both pitch and roll interconnections. A listing of the individual weights of the pitch interconnection components is shown in Table 1. As listed, the largest weight increases are due to the modified dampers and the pressure equalizer. The additional weight for the roll interconnection is relatively low since the modified dampers would already have been added for pitch interconnection.

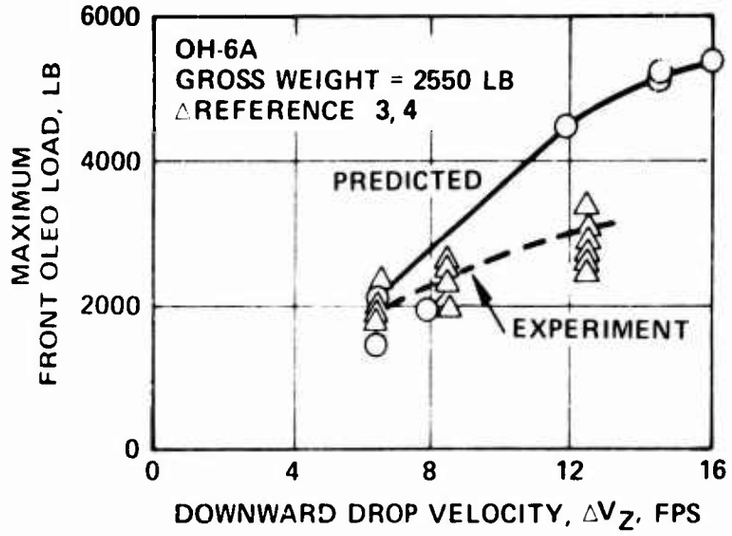

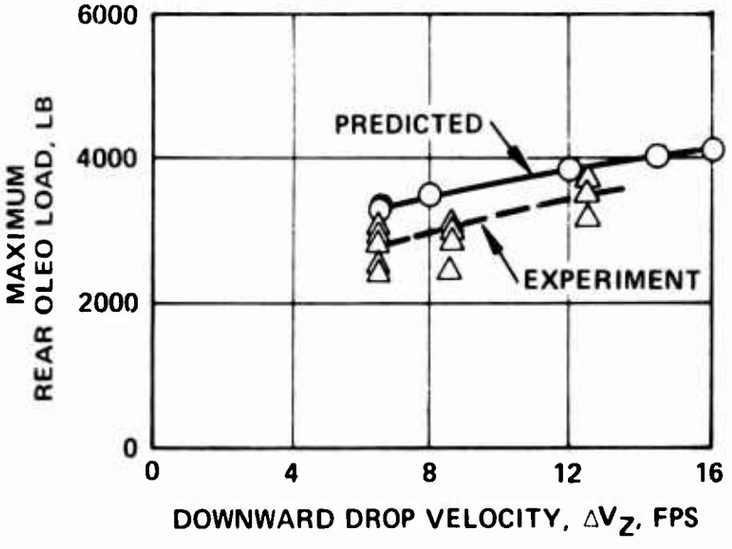

Figure 9. Comparison of Predicted and Experimental Oleo Loads as a Function of Drop Velocity for the OH-6A

TABLE 1. WEIGHT SUMMARY COMPARISON BETWEEN THE BASIC OH-6A AND THE INTERCONNECTED LANDING GEAR

Item	Basic OH-6A Weights, lb	Interconnect Landing Gear Weights, lb	Weight Change, lb
Pitch Interconnection			
Skids	18.3	18.3	0
Abrasion Shoes	3.2	3.2	0
Struts - Drag (4)	4.3	4.3	0
Struts - Side (4)	19.7	22.3	+ 2.6
Dampers (4)	6.4	17.2	+10.8
Fittings - Body	7.8	7.8	0
Fairings - (4)	5.7	7.6	+ 1.9
Misc. Attachment Parts	1.4	1.4	0
Surge Reservoir, lower (4) 2 per side	0	4.0	+ 4.0
Surge Reservoir, upper (2) 1 per side	0	3.0	+ 3.0
Pressure Equalizer (2) 1 per side	0	5.4	+ 5.4
Dual Flow Valve (4) 2 per side	0	2.2	+ 2.2
Air Charging Valve (6) 3 per side	0	1.2	+ 1.2
Plumbing	0	2.6	+ 2.6
Attach Hardware	0	2.0	+ 2.0
Fluid (Hydraulic)	0	5.2	+ 5.2
Subtotal, Pitch Interconnection	66.8	107.7	40.9
Roll Interconnection			
Pressure Equalizer (2)	-	5.4	+ 5.4
Plumbing	-	.8	+ .8
Subtotal, Roll Interconnection		6.2	6.2
Total System Weight Per Aircraft	66.8	113.9	+47.1

INTERCONNECTED LANDING GEAR DEFINITION

The detailed interconnected landing gear system described previously can be designed to have any particular system stiffness and damping. A dynamic analysis has been made of the OH-6A under a severe autorotational landing, and optimum interconnection stiffness and damping values have been defined. For the OH-6A, these values are 150,000 in.-lb/radian and 15,000 $\frac{\text{in.-lb}}{\text{radian/sec}}$ for stiffness and damping, respectively. These values are expressed in radian spring terms due to computer simulation requirements. The equivalent linear spring values are approximately 103 lb/in. and 10.3 $\frac{\text{lb}}{\text{in./sec}}$.

Similar interconnection spring values could be derived for any other helicopter using either a skid or wheel type landing gear. For purposes of this study, the OH-6A is used as the baseline, but the results apply generally to any helicopter.

The selection of the interconnection spring values for the OH-6A is presented in the following section.

Analysis Used

The dynamic characteristics of the interconnection system were analyzed using a computer simulation of a helicopter landing gear. The computer simulation was developed for a conventional OH-6A and modified to represent the interconnected landing gear system.[1] The simulation is described in detail in Appendix A. Available experimental data from landing gear drop tests were used to assist in developing and in verifying the initial computer simulation for the basic OH-6A landing gear. As presented in Appendix A, a comparison of calculated and measured landing gear behaviors indicates that the computer program represents the test values quite well.

---

[1] Currier, E.J., et al, PRELIMINARY DESIGN AND ANALYSIS REPORT, REDUCTION OF VULNERABILITY TO TAILBOOM/BLADE STRIKES, Hughes Tool Company - Aircraft Division Report 369-V-3603, October 1970.

Design Conditions

The helicopter autorotational landing condition used to define the optimum interconnection constraint characteristics was selected to be representative of landing conditions during which blade/tailboom contacts occur. A review of the available flight test data indicated that a nose-up attitude coupled with high vertical contact velocity is the condition during which blade/tailboom contact occurs.[2] In one flight case examined, a high vertical contact velocity was not accompanied with a nose-up attitude and blade/tailboom contact did not occur. Forward velocity magnifies the effect of the nose-up landing attitude but is usually not found with higher nose-up attitudes. Consequently, only vertical velocity and large nose-up attitudes were used to determine the optimum interconnection spring characteristics. The effect of forward speed was then examined for those optimum characteristics.

For design purposes, an autorotational landing condition of 10-degrees nose-up pitch attitude and 6.55-feet-per-second vertical contact velocity was used. The pitch attitude is representative of flight data, and the vertical contact velocity represents a limit energy absorption drop for the basic OH-6A landing gear.

In addition to the helicopter attitude during autorotation, main rotor control movement following touchdown contributes significantly to blade/tailboom contact. Flight records indicate that the initial pilot reaction during a nose high autorotation is to pull the controls back in reaction to the helicopter nose down pitching motion. This has been shown to be an important part of blade/tailboom contact. This blade motion is not simulated in the computer model, which accounts for only the decay of main rotor lift following touchdown. The omission of blade flapping motions and the moments incident thereto affects the resultant airframe motions by less than 5 percent. Therefore, they are neglected in the computer analysis. An estimate of blade location is made by other means so that the increase in blade/tailboom separation can be assessed.

To facilitate the interconnection constraint definition, the basic OH-6A landing gear configuration was used for both interconnected and non-interconnected cases. Once the constraint stiffness and damping were

---

[2] Amer, K. B., PROPOSED OH-6A PRODUCT IMPROVEMENT PROGRAM TO IMPROVE AUTOROTATION LANDING CHARACTERISTICS, Hughes Tool Company - Aircraft Division Report 369-V-3603P, January 1970.

selected, the effects of extending the cross tube length were examined and shown to have little effect on the helicopter pitching behavior with time.

Interconnection Definition

Using the design autorotational condition, a variety of interconnection system stiffnesses and dampings were simulated in the computer program. The objective was to determine the values that achieve the maximum reduction in the helicopter nose-down pitching velocity. The analytical studies indicate that there is a direct correlation between minimum pitching velocity and the maximum interconnection extension, as shown in Figure 10. There, maximum interconnection movement is presented as a function of pitch velocity for a wide range of interconnection stiffnesses and dampings. The interconnection movement shown is the linear distance traveled by the cross tube sleeve/damper juncture at the cross tube elbow. As can be seen, the larger the interconnection travel (and hence the faster the front skid contacts the ground), the lower the resulting pitching velocity. However, as presented in the detail design, the OH-6A pilot seat location limits the amount of interconnection travel available to approximately 1.74 inches. For the initial design, it was decided to choose the values of interconnection dampings and spring constants that did not exceed this geometric limit. Using this as a criteria, the analytical interconnection travel as a function of damping was examined and is presented in Figure 11. As shown in Figure 11, this limit on interconnection travel was achieved by having a damping of approximately 15,000 $\frac{\text{in.-lb}}{\text{radian/sec}}$ and a spring constant of 150,000 in.-lb/radian. These values are now used to represent the interconnection system constraint characteristics. These values do allow slightly more movement than the limit, but it was decided to choose a slightly softer interconnection system so that complete movement would be ensured.

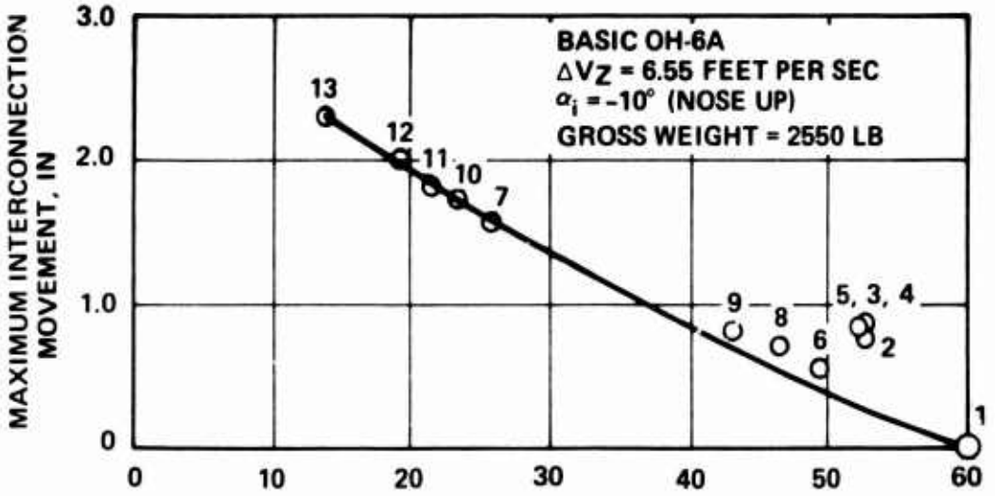

CASE	INTERCONNECTION VALUES	
	DAMPING $\left[\frac{\text{IN-LB}}{\text{RAD/SEC}}\right]$	SPRING $\left[\frac{\text{IN-LB}}{\text{RAD}}\right]$
1	None	None
2	0	720,000
3	200	720,000
4	400	720,000
5	2,400	720,000
6	70,000	720,000
7	0	360,000
8	70,000	360,000
9	70,000	180,000
10	15,000	180,000
11	15,000	150,000
12	15,000	100,000
13	10,000	100,000

Figure 10. Variation of Interconnection Movement With Maximum Nose-Down Pitching Velocity

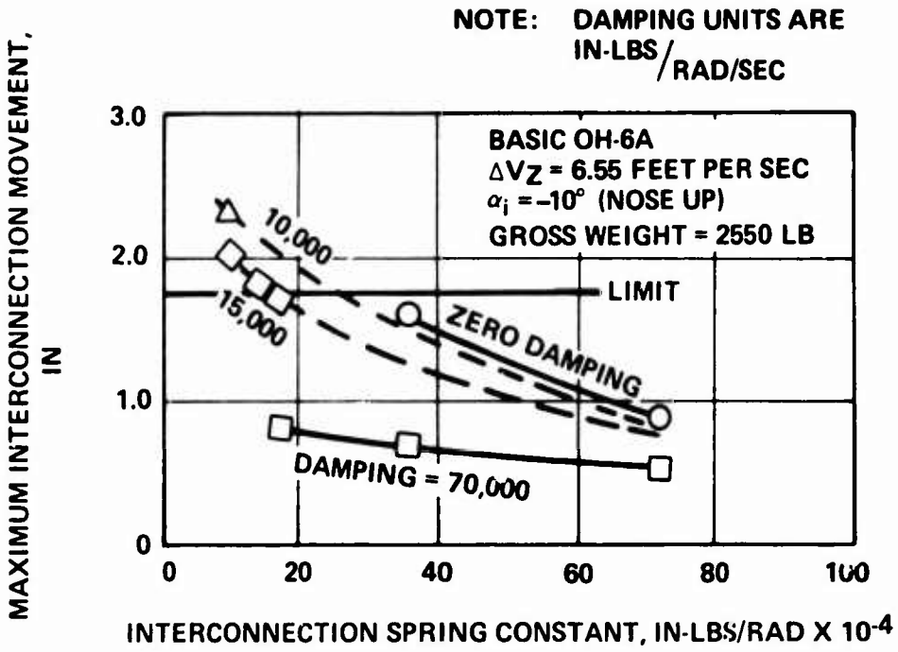

Figure 11. Variation of Interconnection Movement with Interconnection Spring Constant and Damping

INTERCONNECTED LANDING GEAR CAPABILITIES

The interconnected landing gear has been examined for its effect on helicopter behavior during autorotational landings at limit and maximum energy velocities with extreme nose-up and roll attitudes. The analysis shows that violent post-impact helicopter behavior is reduced and that the prospect of blade/tailboom impact is reduced dramatically. The landing gear interconnection per se does not increase maximum downward velocity capability. However, the increased cross tube length (and subsequent increased ground clearance) does significantly increase the maximum downward velocity capability.

Blade/Tailboom Separation

An interconnection system with the optimum constraint characteristics and geometry changes described previously does reduce the nose-down pitch angle and pitching velocity that occur during an autorotational landing, as shown in Figure 12. As can be seen, the interconnection system has only pitched over 3 degrees in the first quarter of a second while the basic OH-6A has pitched over more than 9 degrees. This results in a 60-percent reduction in maximum pitching velocity.

When forward speed is present during an autorotational landing, the interconnection system reduces the pitch angle and pitching velocity but the reductions are not as large as in the case of autorotation without forward speed. The analytical pitch angle and the pitching velocity are shown plotted versus time in Figure 13 for the design condition with forward velocity present. The maximum pitching velocity is reduced from 80 to 62 feet per second and the build-up to that maximum is double the time required by the basic OH-6A. Although these changes in landing behavior are not as large as in a pure vertical impact, they are as significant in that they eliminate blade/tailboom contact during a landing condition similar to an actual landing where blade/tailboom contact was recorded. In the analytical method, forward velocity is simulated by a rearward ground friction force proportional to the normal force at the skid. Comparison of calculated and experimental landing behavior of the basic OH-6A indicates that these cases simulate approximately 30 knots forward speed.

The reductions in pitch angle and pitch velocity due to interconnection cause a dramatic increase in blade/tailboom separation and reduce the probability of blade/boom contact. Blade/tailboom separation is shown

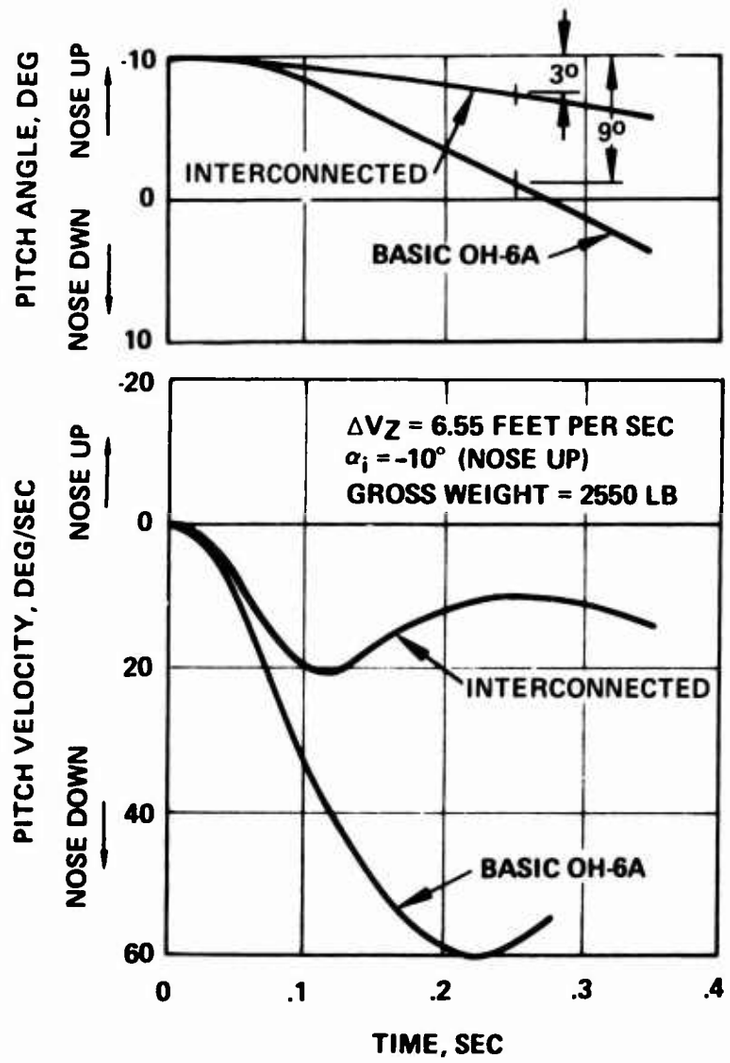

Figure 12. Effect of Interconnected Landing Gear on Pitch Angle and Velocity for a 6.55-foot-per-second Vertical Drop

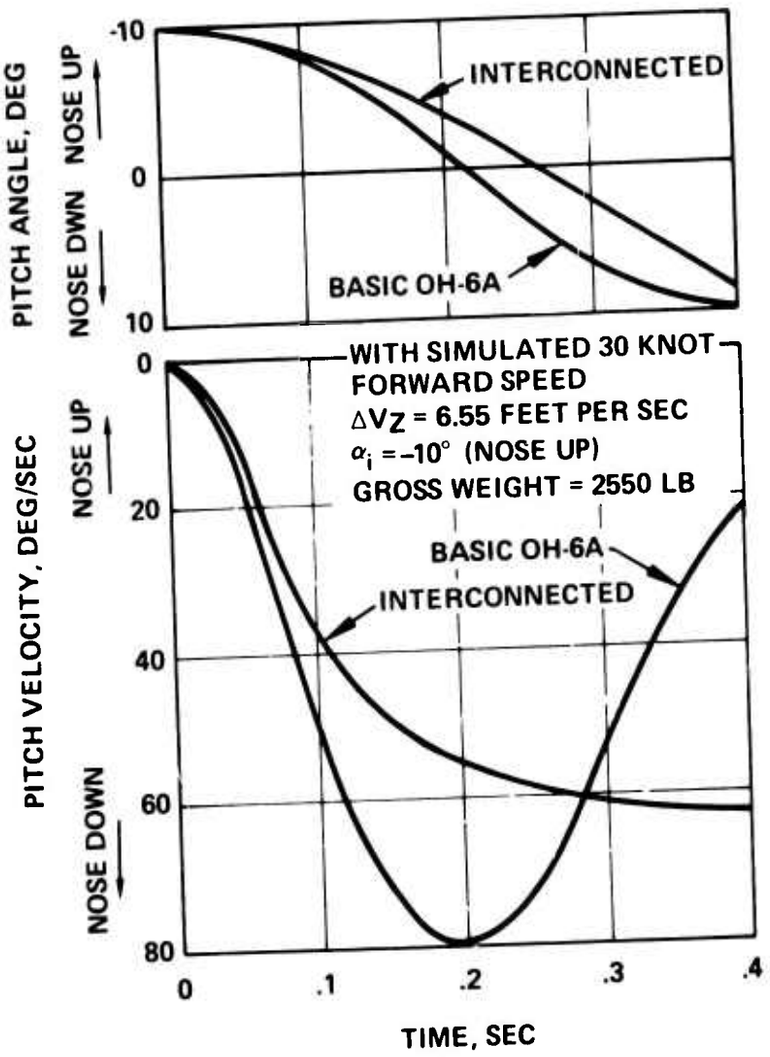

Figure 13. Effect of Interconnected Landing Gear on Pitch Angle and Velocity for a 6.55-foot-per-second Vertical Drop with Simulated 30 knot Forward Speed

in Figure 14 for the interconnected and basic OH-6A landing gears with and without forward velocity. (The definition of blade/tailboom separation is presented in Appendix B.) The interconnection of the landing gear increases separation sevenfold for autorotation without forward speed and eliminates blade/tailboom contact for autorotation with forward speed. The autorotation case with forward speed is similar to an actual landing case where blade/tailboom contact was recorded.

The analysis has demonstrated that given the proper stiffness an interconnected landing gear can dramatically increase blade/tailboom separation and helicopter controllability during autorotational landings. These are general results that can be applied to any helicopter landing gear. For wheeled landing gear, each wheel should be independently movable since they are not interconnected by a skid. For skid gears without dampers, an interconnected landing gear could be designed by installing a linear motion actuator on each cross tube and interconnecting them fore and aft. To provide free motion, a pivot may also be required.

The analysis indicates that increases in autorotational landing controllability are shown with the landing gear interconnected in roll. As shown in Figure 15 for the limit energy absorption drop of 6.5 feet per second and a 10-degree roll attitude, the roll interconnection reduces the maximum roll velocities by twenty percent and makes the helicopter approach a level attitude without overshooting. This effect will greatly reduce the pilot's effort during a tilted-roll autorotational landing.

As will be shown in a later section, the most significant effect of roll interconnection is to increase the ground resonance margins over that of the basic OH-6A.

Energy Absorption Capabilities

The interconnected landing gear was evaluated using the landing gear provisions of MIL-STD-1290 to determine its impact and energy absorption capabilities. The basic OH-6A landing gear was examined and compared to the interconnected landing gear.

In essence, the MIL-STD-1290 specifications require that the aircraft system be designed to prevent occupant injuries during crash impacts of the severity of up to 42-feet-per-second downward vertical velocity. Specifically, the landing gear must be capable of decelerating the aircraft at normal gross weights from 20-feet-per-second downward vertical velocity without allowing the fuselage to contact the ground. The aircraft structure except the rotor blades and the landing gear shall be flightworthy after this impact.

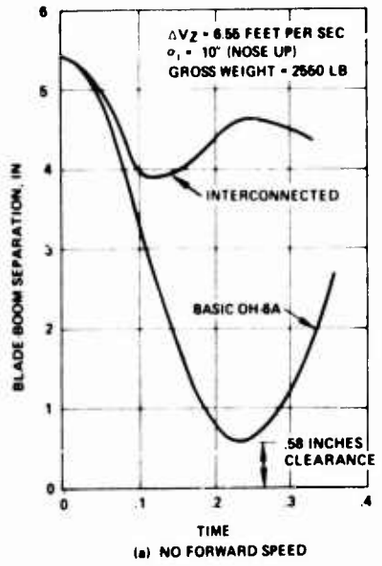

(a) NO FORWARD SPEED

(b) WITH FORWARD SPEED

Figure 14. Effect of Interconnected Landing Gear on Blade/Tailboom Separation

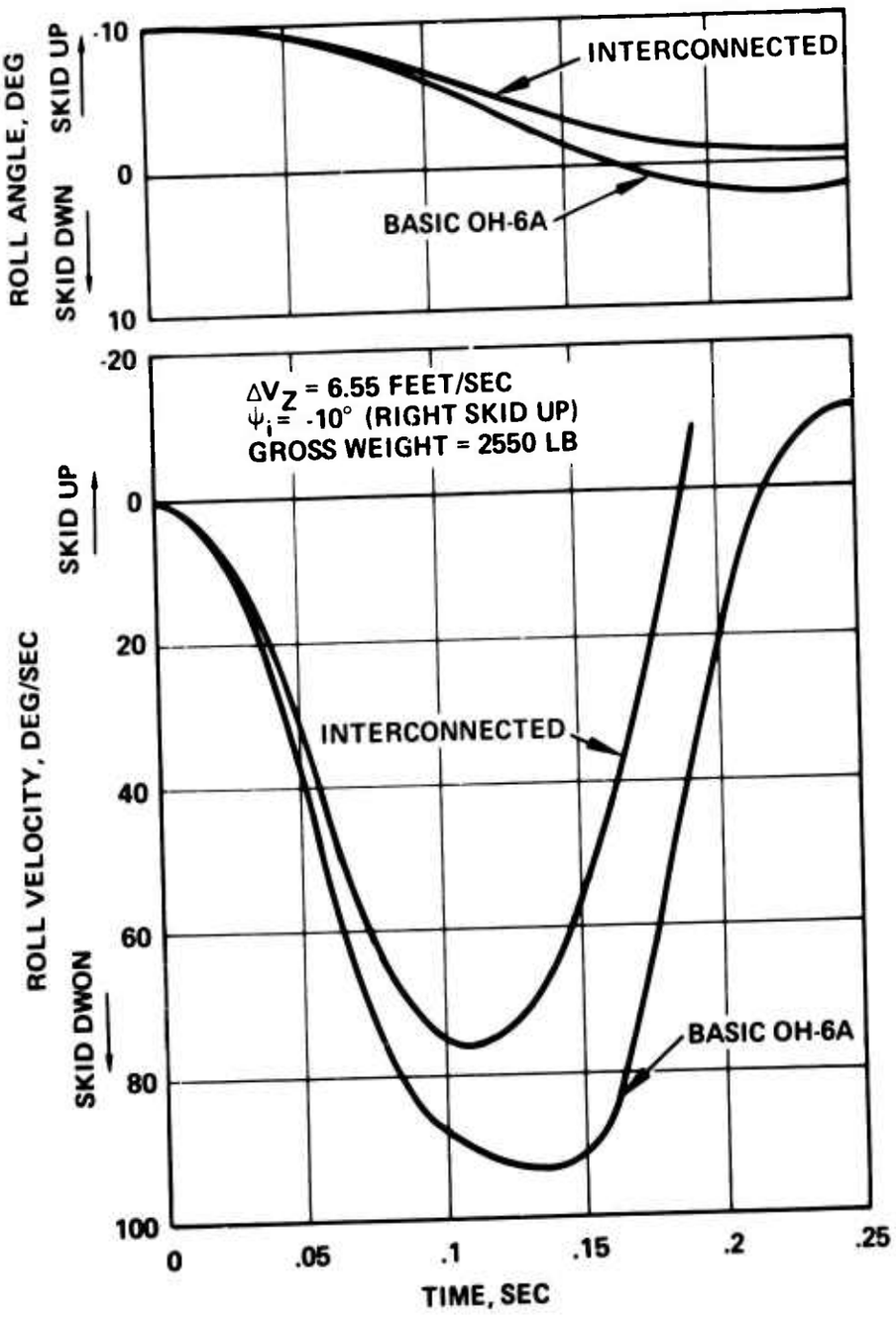

Figure 15. Effect of Landing Gear Interconnection on Roll Angle and Velocity for a 6.55-foot-per-second Vertical Drop

As shown in Figure 16 for a 10-degree nose-up attitude, the analysis indicates that the maximum downward vertical velocity is 14.5 feet per second for the basic OH-6A and 17.5 feet per second for an OH-6A equipped with the interconnected landing gear. The MIL-STD-1290 requirement is not met by either landing gear, but the interconnected gear shows a twenty-percent improvement towards satisfying the requirement.

This increase in downward velocity capability due to the interconnected landing gear is primarily the result of the increased length of the interconnection cross tube over that of the basic OH-6A. The increased cross tube length is required because the interconnected landing gear does not cause the helicopter to pitch as much during nose-high landings. This increases the blade/boom clearance and reduces pilot effort during autorotational landings but also keeps the tail skid closer to the ground. This can be seen in Figure 16. The basic OH-6A is limited in downward velocity by fuselage/ground contact while an OH-6A equipped with the interconnected landing gear is limited by tail skid contact.

The effect of interconnecting the landing gear without lengthening the cross tube has been examined and is shown in Figure 17 at the maximum downward velocity for the basic OH-6A. The fuselage clearance for both the interconnected and basic landing gear is the same, just touching the ground. However, the tail skid of the interconnected landing gear has four inches less clearance and has impacted the ground by approximately two inches. Additional tail skid clearance could be achieved, without lengthening the cross tube, by shortening the lower vertical stabilizer on the interconnected landing gear helicopter. However, this would require aerodynamic redesign of the OH-6A, which was considered to be needlessly complex. The more straightforward approach of lengthening the cross tube was adopted to provide the additional tail-skid/ground clearance.

The full benefit of the increased ground clearance of the interconnected landing gear is found in a level autorotational landing. In this case, there is little pitch change, and the tail skid does not come close to the ground. The fuselage/ground clearance is the critical parameter, and as shown in Figure 18, the maximum allowable downward velocity is increased from 14.5 feet per second to 19.5 feet per second. This increase is due to the extended length cross tube and to the higher yield strength of the cross tube.

The effect of interconnection on blade/tailboom separation was examined for the OH-6A maximum downward velocity and nose-up attitude and is shown in Figure 19. The interconnection doubles the minimum blade/tailboom clearance for this drop. For the basic OH-6A, blade/tailboom clearance is not as critical as it is at lower downward velocities, as

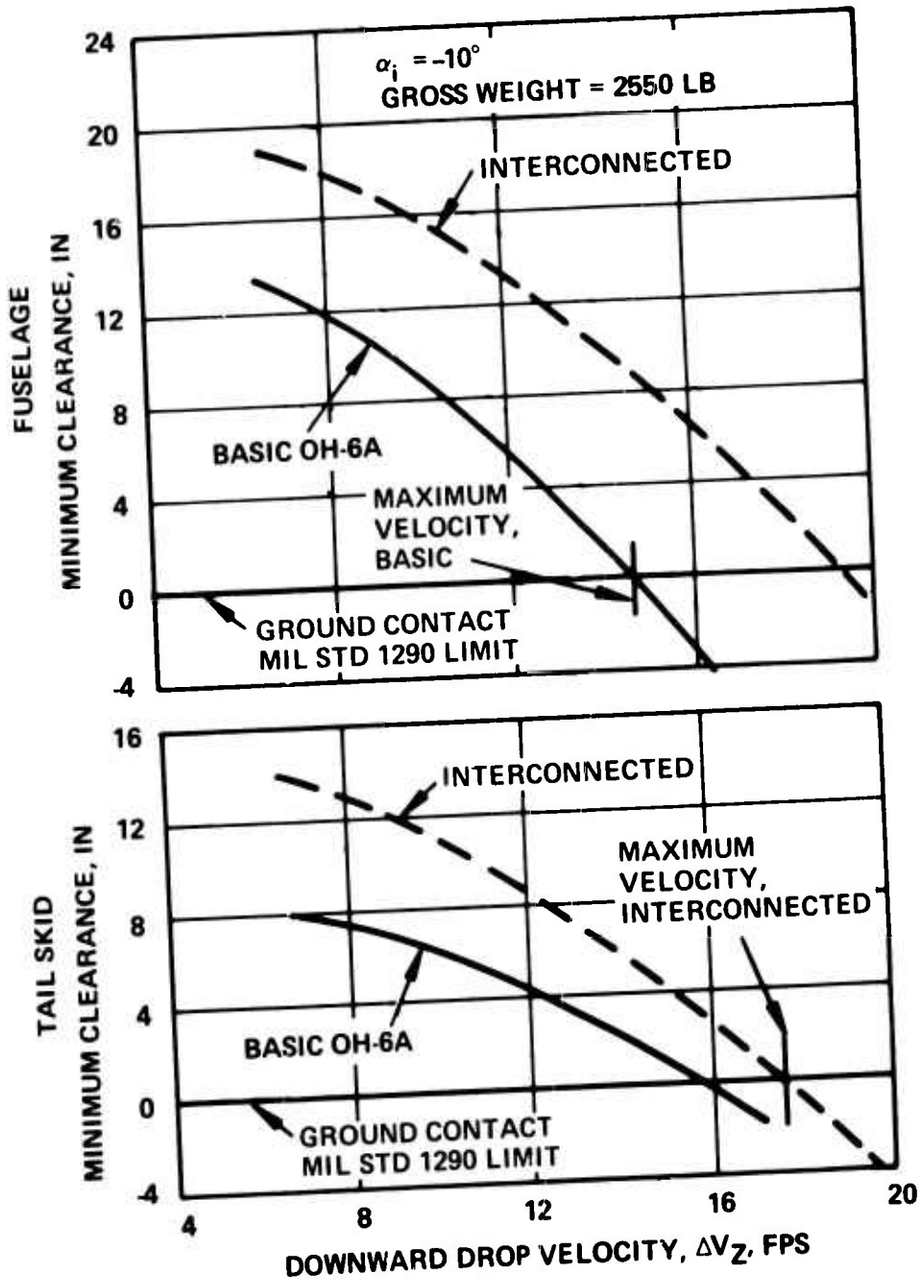

Figure 16. Determination of Maximum Downward Velocity for the Basic OH-6A and the OH-6A Equipped with the Interconnected Landing Gear, α_i = -10°

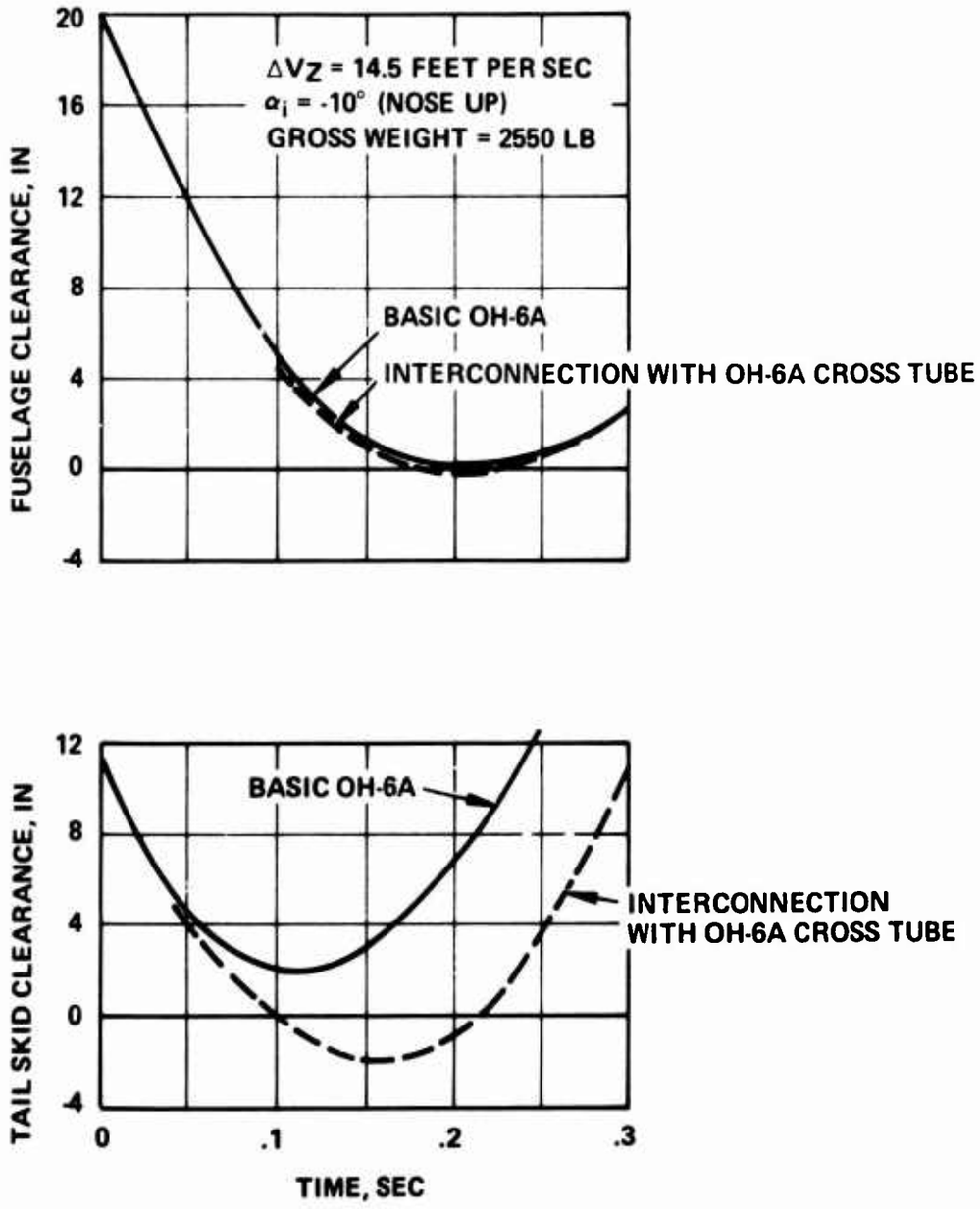

Figure 17. Effect of Pitch Interconnection on Helicopter Ground Clearance for a Standard Length Cross Tube

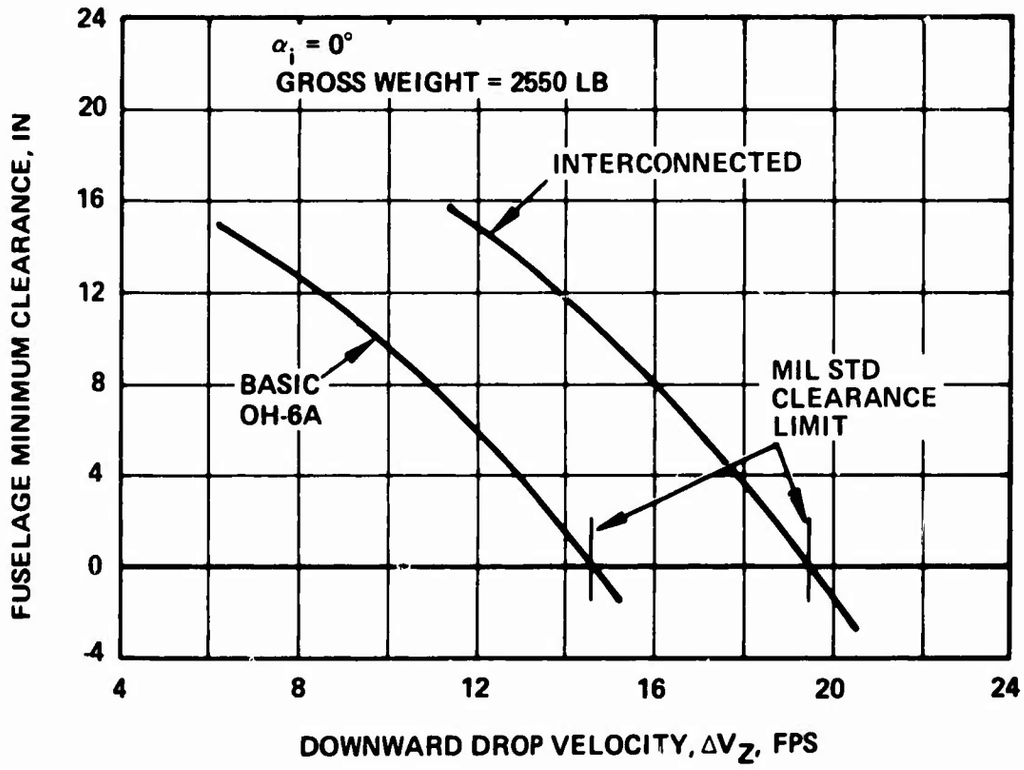

Figure 18. Determination of Maximum Downward Velocity for the Basic OH-6A and the OH-6A Equipped with the Interconnected Landing Gear, α_i = 0°

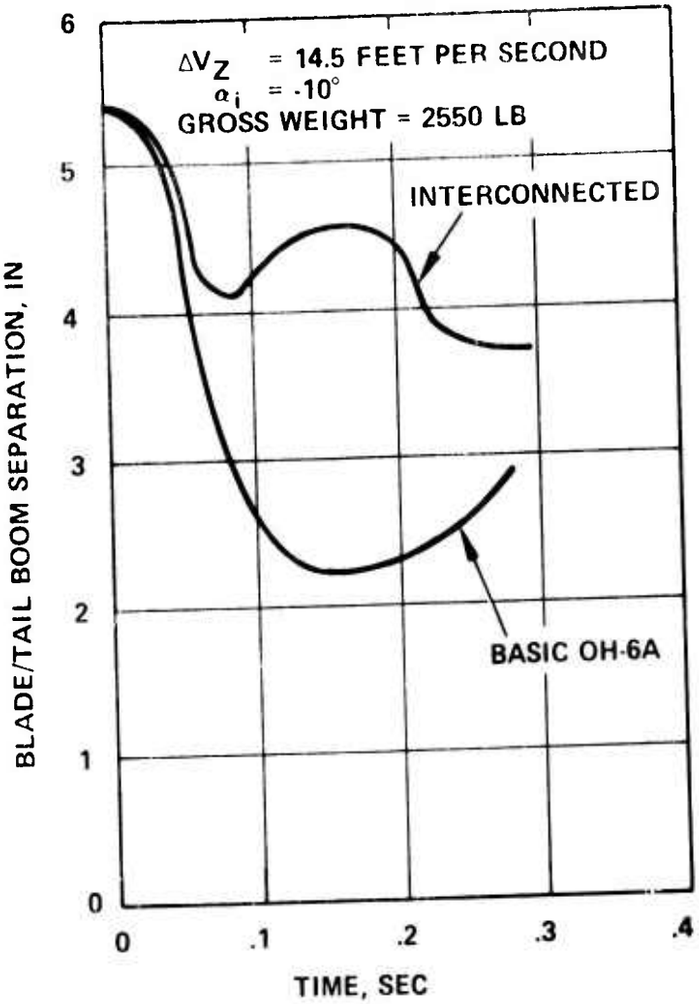

Figure 19. Effect of Landing Gear Interconnection on Blade/Tailboom Separation at the OH-6A Maximum Downward Velocity

shown for 6.5 feet per second (Figure 14). This is due to the yielding of the rear cross tube at the higher downward velocities. The rear cross tube yielding acts in a manner similar to that of the interconnected landing gear. The landing energy is absorbed in yielding instead of generating large pitching moments.

GROUND RESONANCE

This section presents the results of the ground resonance analysis. The benefits of the interconnected landing gear and possible future modifications are discussed. A detailed development of the ground resonance analysis is presented in Appendix C.

The interconnected landing gear considered for analysis is described in the section INTERCONNECTED LANDING GEAR DESIGN and features both pitch and roll interconnection with cross tubes extended 8.32 inches beyond the standard OH-6A cross tube length.

From the ground resonance standpoint, there are two major sources of fuselage damping. One is the interconnection system damping, and the other is the landing gear oleo dampers. For system safety, it was decided to have redundant interconnection and landing gear oleo dampers so that either acting alone would provide the required damping product to satisfy the ground resonance requirements. Consequently, the interconnection system uses the 369H92131 landing gear damper in place of the 369A6340 landing gear damper, used on the basic OH-6A. The 369H92131 landing gear damper was designed for and has been certified for use in a version of the Hughes Helicopter 500C (the commercial version of the OH-6A), which has the cross tubes extended 18 inches. Since the 369H92131 damper provides freedom from ground resonance with an 18-inch cross tube extension, it will provide more freedom from ground resonance with only an 8.32-inch cross tube extension and with failure of the interconnection system. The 369H92131 oleo charge pressure was reduced so as to provide the same oleo position with a 2800-pound gross weight and the 8.32-inch cross tube extension as would be obtained when used with the 18-inch cross tube extension.

Six conditions were considered in the ground resonance analysis, and the description and results are summarized in Table 2. The first two conditions considered were the OH-6A equipped with the interconnected landing gear system at both maximum gross weights and minimum flying weight. The third case considered the interconnected landing gear system at maximum gross weight where the interconnecting system had failed and was inoperative. The fourth condition demonstrated the effect of using the basic OH-6A landing gear oleo damper (369A6340) in the failed interconnection mode instead of the extended cross tube oleo damper

TABLE 2. RESULTS OF GROUND RESONANCE ANALYSIS

	Condition*	Damping Product Ratio** Roll	Damping Product Ratio** Pitch	Natural Frequency, Hz Roll	Natural Frequency, Hz Pitch	Remarks
1.	2800 lb (Max GW) 92131 damper, interconnecting gear	19.1	16.5	1.3	1.2	Interconnected, not bottomed for run-on with friction coefficient of 1.0.
2.	1354 lb (Min FW) 92131 damper, interconnected gear	18.01	21.16	1.4	1.2	
3.	2800 lb (Max GW) 92131 damper, interconnecting gear failed	2.07	9.08	3.0	1.5	Assumes failure of interconnected landing gear system.
4.	2800 lb (Max GW) 6340 damper, interconnecting gear failed	.08	1.63	3.7	1.8	Damping ratio of 1.0 required for stability. Assumes failure of interconnected landing gear system. Charge pressure increased over standard gear to account for 8.32 inch extension.
5.	2550 lb (DGW) basic OH-6A, 6340 damper	.50	-	3.4	-	Baseline condition. Conservative value of oleo damping used, skid friction neglected.
6.	2550 lb (DGW) 6340 damper shake test, basic OH-6A	1.6	-	3.4	-	Experimental simulation of baseline condition (condition 5). Includes skid friction (from Page IVB of Reference 7).

*Zero surface friction was used for all conditions except where noted.

**Damping Product Ratio = $\frac{\text{damping available}}{\text{damping required}}$

Value of one required to prevent ground resonance

(369H92131). The fifth and sixth conditions are analytical and experimental results of the same condition for the basic OH-6A and demonstrate the conservative nature of the analytical model. Zero surface friction was used in the analysis for conditions 1 through 5 so that there would be no damping from the scrubbing of the landing gear skid on the ground. The experimental shake test (condition 6) simulated zero surface friction by using teflon skid shoes on greased steel plates.

The analysis indicates that the interconnected landing gear with the 369H92131 oleo dampers provides more than ample damping to preclude ground resonance. This can be seen in Table 2 for both maximum gross weight (condition 1) and minimum flying weight (condition 2). No problems with the bottoming of the interconnection system due to run-on-landings or aft tilting of the fuselage should be encountered because the skid gear provides most of the pitch stiffness when the oleos are interconnected in pitch. The damping products remain more than adequate even with a failure of the interconnection system, as shown in condition 3, Table 2. In this condition, the critical roll damping product ratio is over twice the ratio required for stability using conservative isotropic and frictionless assumptions.

The basic OH-6A landing gear damper (369A6340) was shown to be inadequate for use in the interconnected landing gear system. A comparison of conditions 3 and 4 of Table 2 shows that substitution of the basic OH-6A damper reduces the critical roll damping ratio to a dangerously low level with interconnection failure at maximum overload conditions. This is because of the increased stiffness and lower damping in combination with the cross tube extension.

The conservative nature of the analysis is indicated by the comparison of the shake test results (condition 6, Table 2) and the analysis using the shake test parameters (condition 5). The analysis indicates instability (damping product ratio less than one) using the conservative assumption of isotropic pylon supports and ignoring surface friction. However, the shake test, which also uses the conservative isotropic assumption, shows stability with a damping product ratio higher than that predicted by a margin of one.

As has been shown, the interconnected landing gear system has at least four times the damping product ratio as the basic OH-6A even with interconnection failure. It also has twice the most conservative requirements for stability. In addition, the analysis has been shown to be conservative by a damping ratio margin of one. Consequently, it would appear that there is adequate margin to reduce the blade damping requirements. This

would permit widening the first-stage damping and eliminating one or more intermediate stages in the blade dampers. By providing more first-stage discs, damper adjustment torque and thus disc wear could be reduced, resulting in reduced maintenance costs and vibration problems due to "damper beat."

The simplification of the oleos by the elimination of the anti-extension spring and the widening of the operating temperature range may also be possible. The anti-extension spring and the cold/warm weather oleos are required to prevent deactivation of the oleos for light on the skids conditions. Since proper pilot procedure, immediate lift-off, makes this a redundant requirement which will be more than adequately fulfilled with the roll interconnect functioning, it should be possible to increase the "warm weather" charge pressure to prevent oleo bottoming at a lower temperature and to eliminate the anti-extension spring.

LIFE-CYCLE COSTS

A cost effectiveness study has been conducted to determine the impact of the improved, interconnected landing gear design on the life-cycle cost (LCC) of an OH-6A fleet. For study purposes, an OH-6A life and deployment model was chosen that is identical to the model used to determine YAH-64 AAH life-cycle costs. The total aircraft inventory assumed in the model is determined using a production rate which produces 472 aircraft over a seven-year period and then using an equivalent retirement rate fifteen years later. When the inventory falls below 100 aircraft, the fleet is retired. Flight schedules are based on peacetime levels of 240 flight hours per year, and maintenance schedules are based on wartime levels of 840 flight hours per year. The high maintenance loading is an attempt to simulate wartime operational availability during peacetime and is considered conservative. The life and deployment model chosen for the OH-6A does not reflect current OH-6A use. Rather, the model was chosen to be representative of helicopters currently entering service. In this way, a meaningful assessment of the cost savings of installing the interconnected landing gear system on current helicopters could be determined.

The two major segments of the LCC model are investment costs and operations and support (O&S) costs. The major elements that determine the investment costs are the design-to-unit-cost (DTC) and nonrecurring cost, required for the interconnected landing gear. The DTC is estimated to be $1440 in 1972 dollars and includes both pitch and roll interconnection. Also included in investment cost is $220,000 of nonrecurring costs associated with the interconnected landing gear development. The major elements of the operation and support (O&S) costs are the increased maintenance due to the interconnected landing gear and the reduction in costs due to increased blade/tailboom clearance which is based on the frequency of tailboom strikes. The increased maintenance was estimated using the reliability and maintainability techniques developed for the YAH-64. Blade/tailboom strike frequency data were obtained from USABAAR. These data indicate that blade/tailboom strikes occur at a rate of approximately one per 5600 flight hours at a cost of $5.10 per flight

hour (1972 dollars). It is estimated that the interconnected landing gear would eliminate 80 percent of these blade/tailboom strikes. [1]

The life-cycle cost analysis shows that the improved, interconnected landing gear would result in a $2,400,000 LCC savings in 1972 constant dollars over a period of 15 years (1972 dollars are used as a baseline and are consistent with YAH-64 cost model practice). This represents a benefit to cost ratio of over 2:1. The analysis also shows that these savings are relatively insensitive to increases in DTC. A 50-percent increase in DTC caused a decrease in LCC savings of only 14 percent.

---

[1] Currier, E. J., et al, PRELIMINARY DESIGN AND ANALYSIS REPORT, REDUCTION OF VULNERABILITY TO TAILBOOM/BLADE STRIKES, Hughes Tool Company - Aircraft Division Report 369-V-3603, October 1970.

CONCLUSIONS

1. Interconnection of the front and rear supports of a skid-type landing gear significantly reduces the maximum nose-down pitching angles and velocities that occur during autorotational landings. This results in a more controllable autorotational landing.

2. The reduction in nose-down angles and velocities increases blade/tailboom separation. The increase in separation is larger in a pure vertical landing than in a landing with forward speed. Although the increase in blade/tailboom separation is smaller, the contribution of the interconnected landing gear during forward speed autorotation landings is significant because it eliminates blade/tailboom contact in a landing where contact has been recorded.

3. The interconnected landing gear increases the maximum downward velocity capability of the baseline helicopter by 3 feet per second in a nose-high landing and 5 feet per second in a level landing. These increases result from additional ground clearance required by the interconnection system.

4. The lateral interconnection of the landing gear produces the same increase in helicopter controllability during autorotation with roll as does the fore and aft interconnection in pitch. The use of lateral interconnection increases ground resonance margins by reducing the roll natural frequency. This can be used to increase helicopter ground resonance stability margins, in decreasing blade damping about the lead-lag hinge, or possibly in widening the oleo temperature operating range and allowing design simplification by eliminating the anti-extension spring.

5. The redundancy of the interconnection system and oleos increases helicopter reliability.

6. A life-cycle costs analysis of the interconnected landing gear indicates that it would generate a cost savings of over two times the initial cost.

RECOMMENDATIONS

1. It is recommended that an interconnected landing gear be produced and tested under simulated autorotational landing conditions.

2. A preliminary design of an interconnected wheel type landing gear should be developed for AAH and UTTAS type helicopters.

REFERENCES

1. Currier, E.J., et al, PRELIMINARY DESIGN AND ANALYSIS REPORT, REDUCTION OF VULNERABILITY TO TAILBOOM/BLADE STRIKES, Hughes Tool Company - Aircraft Division Report 369-V-3603, October 1970.

2. Amer, K.B., PROPOSED OH-6A PRODUCT IMPROVEMENT PROGRAM TO IMPROVE AUTOROTATION LANDING CHARACTERISTICS, Hughes Tool Company - Aircraft Division Report 369-V-3603P, January 1970.

3. Magula, A.W., DROP TESTS OF IMPROVED LANDING GEAR (HTC-AD M30245 KIT) FOR MODEL 369A HELICOPTERS (USING 369A6300 DAMPERS), (GROSS WEIGHTS: 2550 LB AND 2800 LB), Hughes Tool Company - Aircraft Division Report 369-BT-3613.

4. Meertens, J., et al, PRELIMINARY STRESS ANALYSIS, MODEL 369C DEMONSTRATOR, Hughes Tool Company - Aircraft Division Report 369-S-8006, August 1971.

5. Currier, E.J., MODEL 369A (OH-6A) HELICOPTER MAIN ROTOR BLADE MOTION STUDY, Hughes Tool Company - Aircraft Division Report 369-GT-8005, September 1969.

6. Conlin, J.F., CALCULATED MASS PROPERTY DATA, HUGHES HELICOPTER MODEL 369A, Hughes Tool Company - Aircraft Division Report 369-W-8003, April 1966.

7. Soltis, S., STRESS ANALYSIS FUSELAGE 369-S-3004, unpublished.

8. Neff, J.R., GROUND RESONANCE SUBSTANTIATION, MODEL 369H SERIES, Hughes Tool Company - Aircraft Division Report 369-V-8006.

9. Mil, M.L., et al, HELICOPTER CALCULATION AND DESIGN, VOLUME II VIBRATIONS AND DYNAMIC STABILITY, National Aeronautics Space Administration TTE-519, May 1968.

APPENDIX A

DESCRIPTION OF ANALYTICAL STUDIES

Analytical studies were conducted with the aid of a high-speed digital computer. The helicopter landing gear was modeled with a system of nonlinear, simultaneous, ordinary, differential equations. A time history was generated from these differential equations using the Adams four-point integration method.

The mathematical model uses one-half the helicopter. This assumes lateral symmetry during the landing. Figure A-1 presents a schematic front view of the landing gear at the instant of impact and after impact. X_2 is the displacement at the landing gear pivot point, and X_1 is the vertical deflection of the cross tube. The deflection of the gear at the ground due to the compression of the oleo is equal to the oleo deflection divided by the mechanical advantage. The deflection of the cross tube is measured in the vertical direction; therefore, the stiffness of the cross beam varies as the gear is compressed. In addition, the ground friction changes the direction of the force on the cross tube, which changes the effective stiffness.

Figure A-2 presents a side view, showing the landing gear at the instant of impact during a nose-up landing.

Figure A-3 presents a schematic view of the oleo cross tube combination. The spring in series with the damper is due to air entrapped in the oil. Figure A-3 also presents the representation used in the analysis. The spring representing the entrapped air was assumed to be in series with the cross tube spring, and the oleo was assumed to be a spring and damper in parallel.

Oleo bottoming is handled by adding a very stiff spring in parallel with the oleo spring and damper. This stiff spring is added when the oleo deflection is equal to the maximum value.

The following equations are used in the analysis:

1. **Summing forces in the vertical direction**

$$\frac{m}{2} \ddot{X}_{C_G} = \frac{W}{2} - \frac{L}{2} - F_{x_f} - F_{x_R}$$

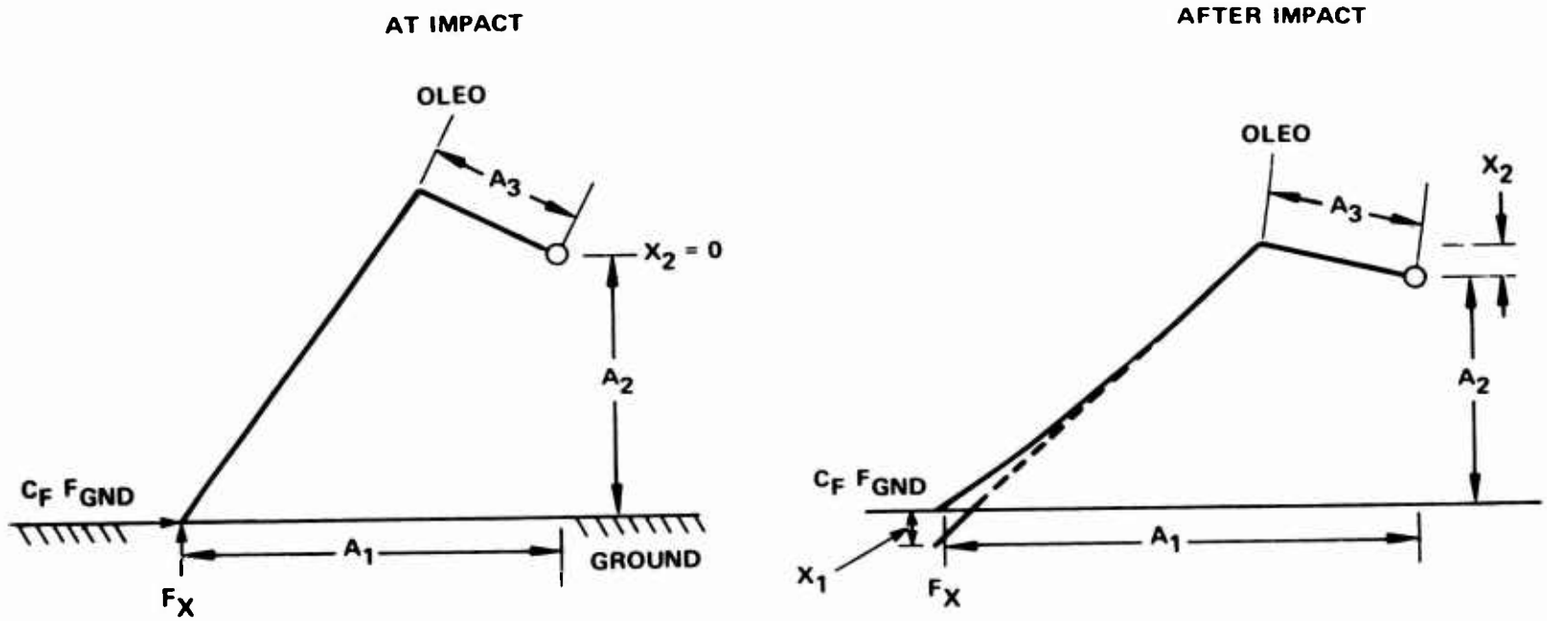

Figure A-1. Schematic Front View of Landing Gear

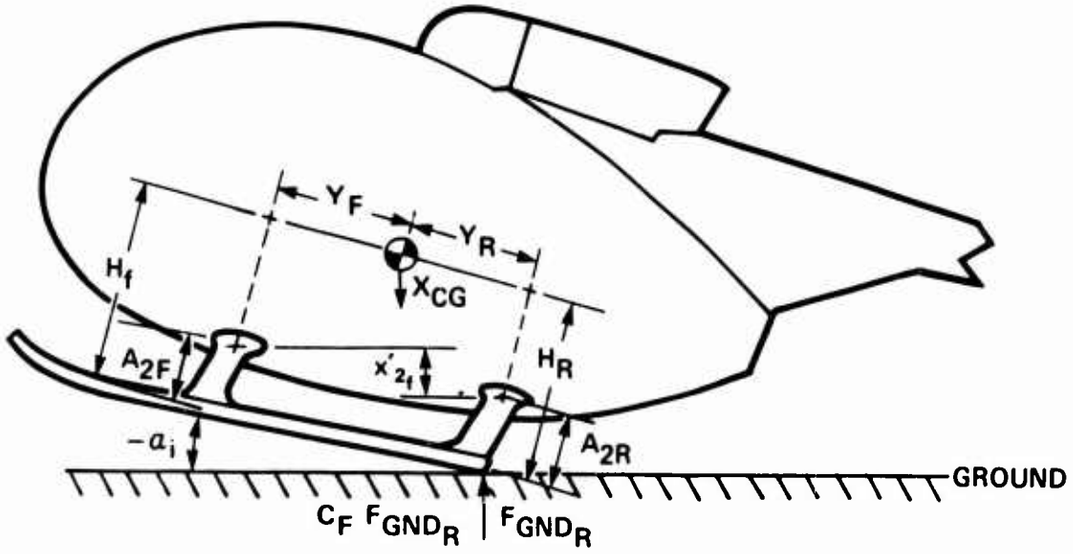

Figure A-2. Side View of Landing Gear

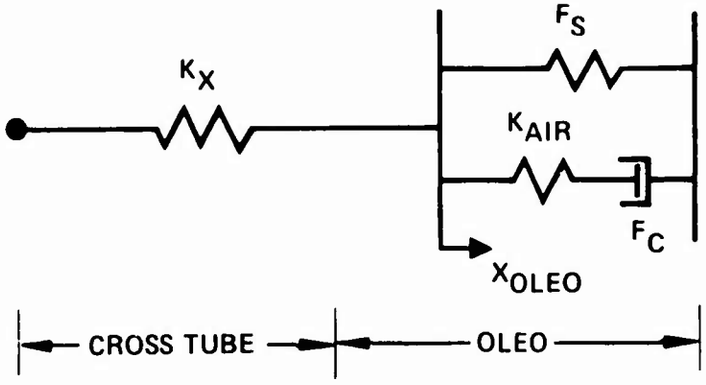

OLEO – CROSS TUBE SCHEMATIC

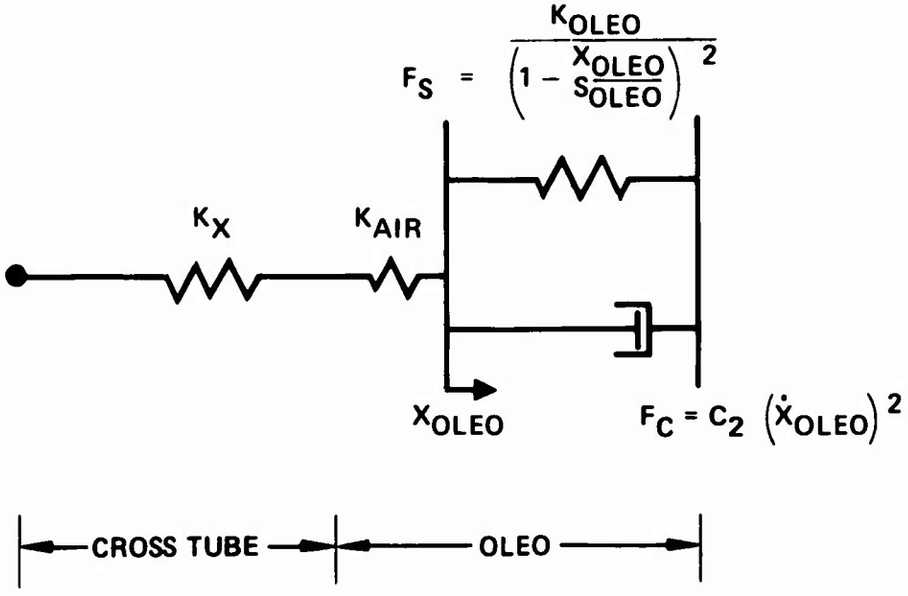

OLEO – CROSS TUBE REPRESENTATION

Figure A-3. Oleo - Cross Tube Representation

2. Summing pitching moment

$$I\ddot{\theta} = F_{Gnd_f} Y_f - F_{Gnd_R} Y_R - C_F F_{Gnd_f} H_F - C_F F_{Gnd_R} H_R$$

3. From Figure A-2

$$X_{2_f} = X_{C_G} - Y_f \sin(\alpha_i - \theta) + X'_{2_f}$$

$$X_{2_R} = X_{C_G} + Y_R \sin(\alpha_i - \theta)$$

4. Differentiate equations in 3

$$\dot{X}_{2_f} = \dot{X}_{C_G} + \dot{\theta} Y_f \cos(\alpha_i - \theta)$$

$$\dot{X}_{2_R} = \dot{X}_{C_G} - \dot{\theta} Y_R \cos(\alpha_i - \theta)$$

5. The force in cross tube as a function of stiffness and deflection

$$F_{x_f} = K_{x_f} X_{l_f}$$

$$F_{x_R} = K_{x_R} X_{l_R}$$

where K_{x_f} and K_{x_R} are functions of C_F and their respective X_{GR}.

6. From Figure A-1

$$F_{oleo_f} = \left(\frac{A_1}{A_3}\right)_f F_{x_f} \mp \left(\frac{A_2}{A_3}\right)_f (C_F F_{Gnd_f})$$

$$F_{oleo_R} = \left(\frac{A_1}{A_3}\right)_R F_{x_R} \mp \left(\frac{A_2}{A_3}\right)_R (C_F F_{Gnd_R})$$

where: - is for a compression stroke
+ is for an extension stroke

7. From Figure A-1

$$\dot{X}_{1_f} = \dot{X}_{2_f} - \dot{X}_{oleo_f} / C_{oleo_f}$$

$$\dot{X}_{1_R} = \dot{X}_{2_R} - \dot{X}_{oleo_R} / C_{oleo_R}$$

8. From Figure A-1

$$X_{GR_f} = X_{2_f} - X_{1_f}$$

$$X_{GR_R} = X_{2_R} - X_{1_R}$$

9. Oleo deflection

$$X_{oleo_f} = C_{oleo_f} X_{GR_f}$$

$$X_{oleo_R} = C_{oleo_R} X_{GR_R}$$

10. From Figure A-3

$$F_{oleo} = \left(\frac{K_{oleo}}{1 - \frac{X_{oleo}}{S_{oleo}}} \right) Exp + C_{2_f} \left(\dot{X}_{oleo} \right)^2$$

11. Coupling force due to skid tube bending and twisting

$$F_c = K_c (X_{1_R} - X_{1_f})$$

12. Ground force

$$F_{Gnd_f} = F_{x_f} - F_c$$

$$F_{Gnd_R} = F_{x_R} + F_c$$

The program was extended to include the interconnection spring and damper in the following manner.

The interconnection spring and damper are assumed to be angular and located halfway between the front and rear cross tubes. The moment is applied to the interconnection arm through the oleos, thus the interconnection sees the oleo force. The equations are:

13. $\dot{\alpha}_{int} = (F_{oleo_R} D_{int} - F_{oleo_F} D_{int} - K_{int} \alpha_{int})/C_{int}$

14. $X_{int} = D_{int} \sin \alpha_{int}$

where: D_{int} = half the distance between front and rear cross tubes

α_{int} = Angle of interconnection spring

K_{int} = Interconnection spring constant

C_{int} = Interconnection damping

X_{int} = Deflection of front and rear cross tubes.

Referring to Figure A-4, the following changes must be made to the previous equations.

In equation 2, the change is

$$H_F = H_{F_{initial}} + X_{int}$$

$$H_R = H_{R_{initial}} - X_{int}$$

In equation 3, the change is

$$X_{2_F} = X_{CG} - Y_f \sin (\alpha_i - \theta) + \dot{X}'_{2_f} + X_{int}$$

$$X_{2_R} = X_{CG} - Y_R \sin (\alpha_i - \theta) - X_{int}$$

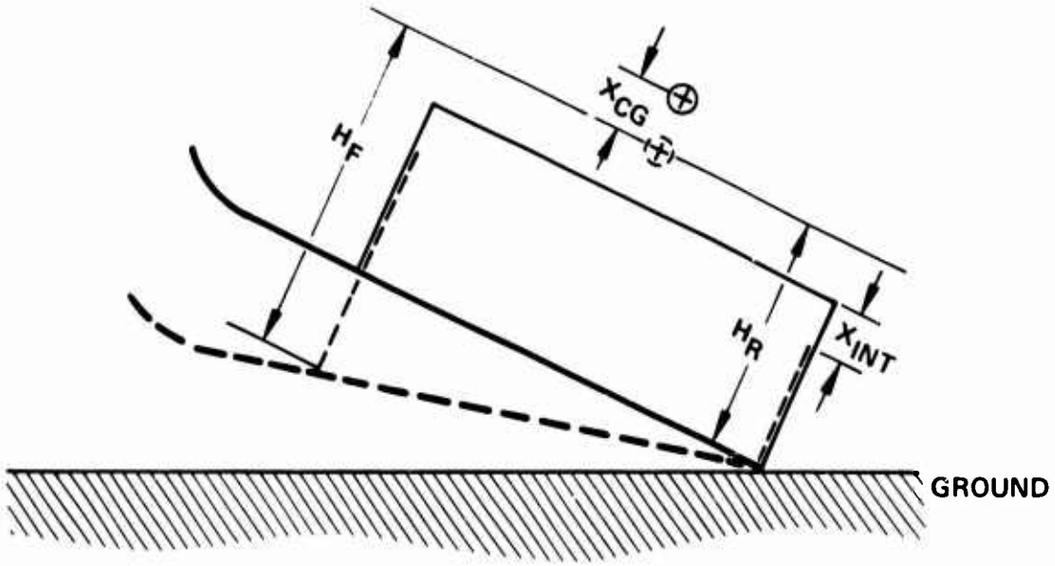

Figure A-4. Landing Gear with Interconnection

The procedure starts at time = 0 at the point of impact. $\ddot{X}_{CG}$ and $\ddot{\theta}$ are obtained from equations 1 and 2. $\dot{X}_2$ is computed using equation 4 after $\dot{X}_{CG}$ has been obtained from the integration $\ddot{X}_{CG}$. $\dot{X}_{oleo}$ is computed from equation 10 and is used in equation 7 to compute $\dot{X}_1$. $\dot{X}_1$ is integrated to obtain X_1 which is used in equation 5 to calculate the cross tube force. $\ddot{\theta}$ is integrated twice to get fuselage attitude.

The yield on the cross tube is handled by setting a maximum yield moment generated by the cross tube force. As the maximum moment is reached and the cross tube yields, the force remains constant. When the gear starts to extend, the deflection due to yielding remains. This is shown in Figure A-5, which is a plot of force vs deflection.

When either the front or the rear gear is off the ground, the cross tube force is equal to the coupling force (equation 11), and the ground force is equal to zero. When this occurs the integration is performed on the oleo velocity $\dot{X}_{oleo}$ in order to obtain the oleo deflection.

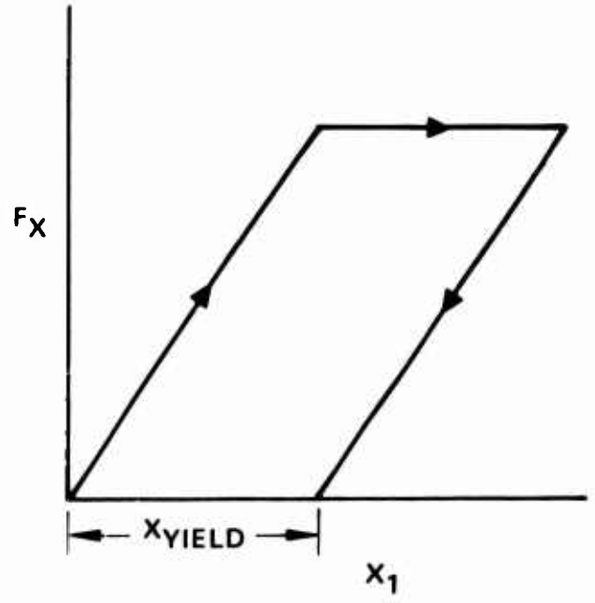

Figure A-5. Cross Tube Force Versus Deflection Showing Yield

A simulation was made of a drop test of a basic OH-6A helicopter.[3] The measured and calculated results of load factor at the CG and pitching velocity about the CG are shown in Figures A-6 and A-7. The magnitude and variation with time of the CG acceleration is predicted accurately. The analysis predicts the general variation with time of the pitching velocity but leads in time and predicts a slightly higher peak pitching velocity than was measured. These discrepancies are attributed to the fact that the frequency response (6 cps) of the pitching velocity recording system was not fast enough to measure a true instantaneous value. Consequently, the measured pitching velocity values reflect an inherent time integration bias which results in an experimental time lag and a lower maximum value than actually occurred.

[3]Magula, A. W., DROP TESTS OF IMPROVED LANDING GEAR (HTC-AD M30245 KIT) FOR MODEL 369A HELICOPTERS (USING 369A6300 DAMPERS), (GROSS WEIGHTS: 2550 LB AND 2800 LB), Hughes Tool Company - Aircraft Division Report 369-BT-3613.

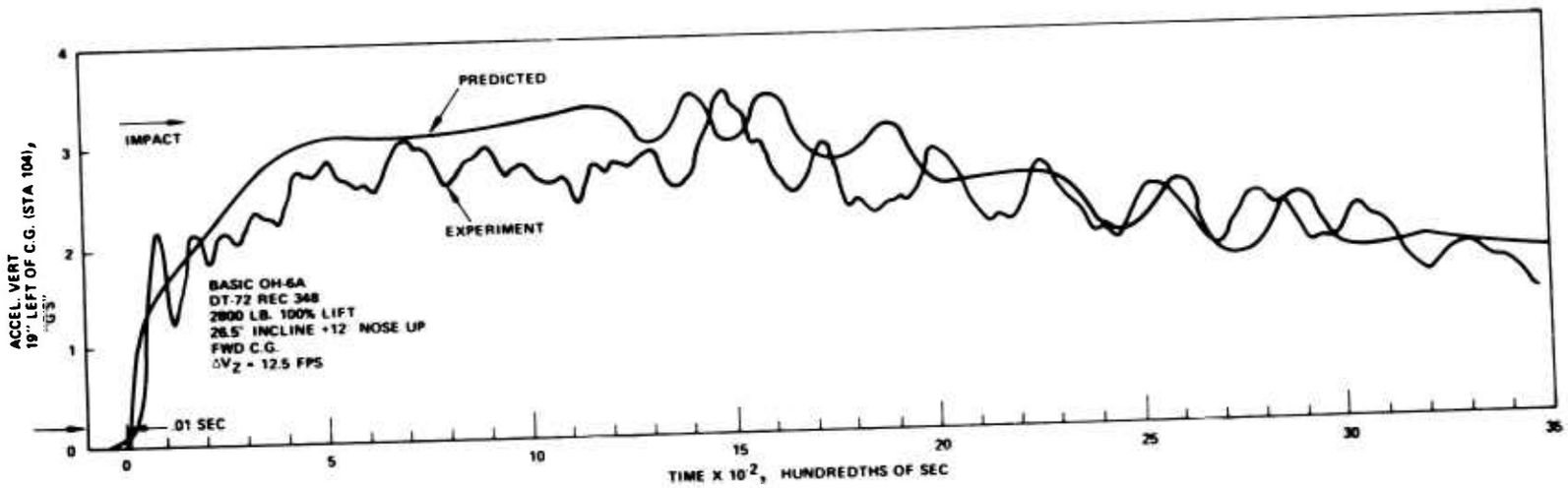

Figure A-6. Comparison of Theoretical and Experimental Vertical Accelerations for the Basic OH-6A

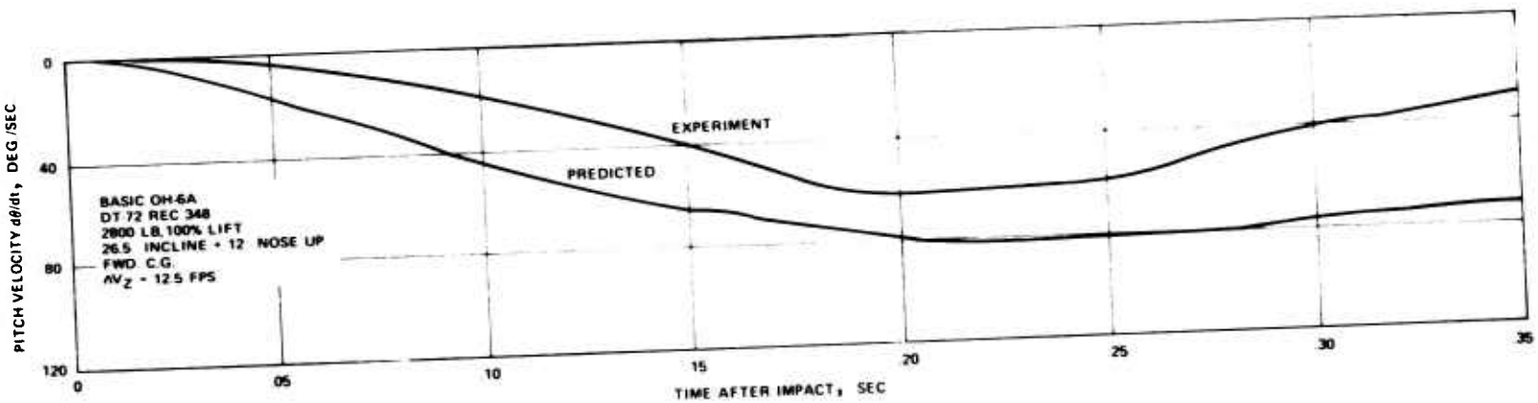

Figure A-7. Comparison of Theoretical and Experimental Pitch Velocities for the Basic OH-6A

APPENDIX B

BLADE/TAILBOOM CLEARANCE

The clearance between the blade and the tailboom has been estimated based on three assumptions.

- During autorotational landing, the pilot must pull all the way back on the controls so that the blade tip path plane is tilted to the extreme rear position. The blade may now have hit the droop stops over the tail.
- Fuselage (and tailboom) pitch angle changes following touchdown are seen by the blade tip path plane as shaft angle changes (i.e., blade angle of attack changes).
- The blade tip path plane will lag those shaft angle changes by a time lag based on the rotor speed and phase angle.

Given the phase and shaft angle input assumptions, the time lag between tailboom angle changes and the blade tip path plane angle is determined by:

$$\Delta t = \frac{\phi}{\Omega}$$

ϕ = phase angle, $\pi/2$

Ω = rotor speed, rad/sec

Using the OH-6A rotor speed, the time lag becomes 0.03 sec. The tailboom pitch angle, $\Delta\alpha_{TB}$, changes with time, t, as a function of the fuselage pitching velocity, $\dot{\alpha}$, such that $\Delta\alpha_{TB} = \dot{\alpha}t$. The blade tip path plane angle, $\Delta\alpha_{BLD}$, changes at the same rate, $\dot{\alpha}$, but lags in time by Δt: $\Delta\alpha_{BLD} = \dot{\alpha}\ (t-\Delta t)$.

Given these two angle behaviors, the separation between blade and the tailboom is given by the following equations:

$$\text{Separation} = H_o - L \sin\left(\Delta\alpha_{TB} - \Delta\alpha_{BLD}\right)$$

$$\text{Separation} = H_o - L \sin\left[\Delta\alpha_{TB}(t) - \Delta\alpha_{TB}\ (t - .03)\right]$$

Where H_o = initial separation = 5.4 inches (Figure 5)

L = distance from helicopter CG to tailboom surface closest to blade

This expression satisfies the qualitative behavior of blade/tailboom separation. As the helicopter pitch over in autorotational landing becomes more rapid, the more probable becomes blade/tailboom contact. At the other limit, if the fuselage pitches very slowly, blade/boom contact becomes unlikely. This was shown experimentally in Reference 5, where, for the OH-6A at rest ($\Delta\alpha_{TB} = \Delta\alpha_{BLD} = 0$), it was impossible to strike the tailboom using only main rotor controls.

---

[5] Currier, E. J., MODEL 369A (OH-6A) HELICOPTER MAIN ROTOR BLADE MOTION STUDY, Hughes Tool Company - Aircraft Division Report 369-GT-8005, September 1969.

APPENDIX C

DETAILED GROUND RESONANCE ANALYSIS

This section presents the details of the ground resonance analysis. The first part details the derivation of the elements used in the complex dynamic model of the fuselage. The second part presents the method of combining these elements into equivalent elements and obtaining the damping product ratios.

The mechanical representation of the mathematical roll/pitch model used in the ground resonance analysis is shown in Figure C-1. The values and description of the elements of this model are given in Table C-1. The derivations of the element values are shown in the appropriate section.

As shown in Figure C-1, the final roll/pitch model is the result of the progressive combination of the damping and stiffness elements of the basic roll, pitch, and bounce model of the helicopter. The complex interaction of the damping and stiffness of the landing gear dampers, the interconnections, and the cross tubes is first reduced to simplified roll and pitch models which replace the series combinations of springs and dampers with equivalent stiffness and damping to represent the pitch and roll models. These two models are simplified again to single degree of freedom models that consider only fuselage roll or pitch moment of inertia (I_ϕ or I_θ), final equivalent hub lateral (roll) or longitudinal (pitch) damping (C_y or C_x), and total roll or pitch stiffness (K_ϕ, K_θ). Natural frequencies and damping can then be determined for any particular combination of landing gear components. For this analysis, the combination of components examined was the basic OH-6A landing gear, the interconnected landing gear with 369H92131 dampers, and the inoperative interconnected landing gear with both the 369H92131 damper and the basic OH-6A damper, 369A6340. The natural frequencies and damping determined are used in a Coleman analysis to determine damping ratio.

The derivation of the element values used in the ground resonance analyses is presented below.

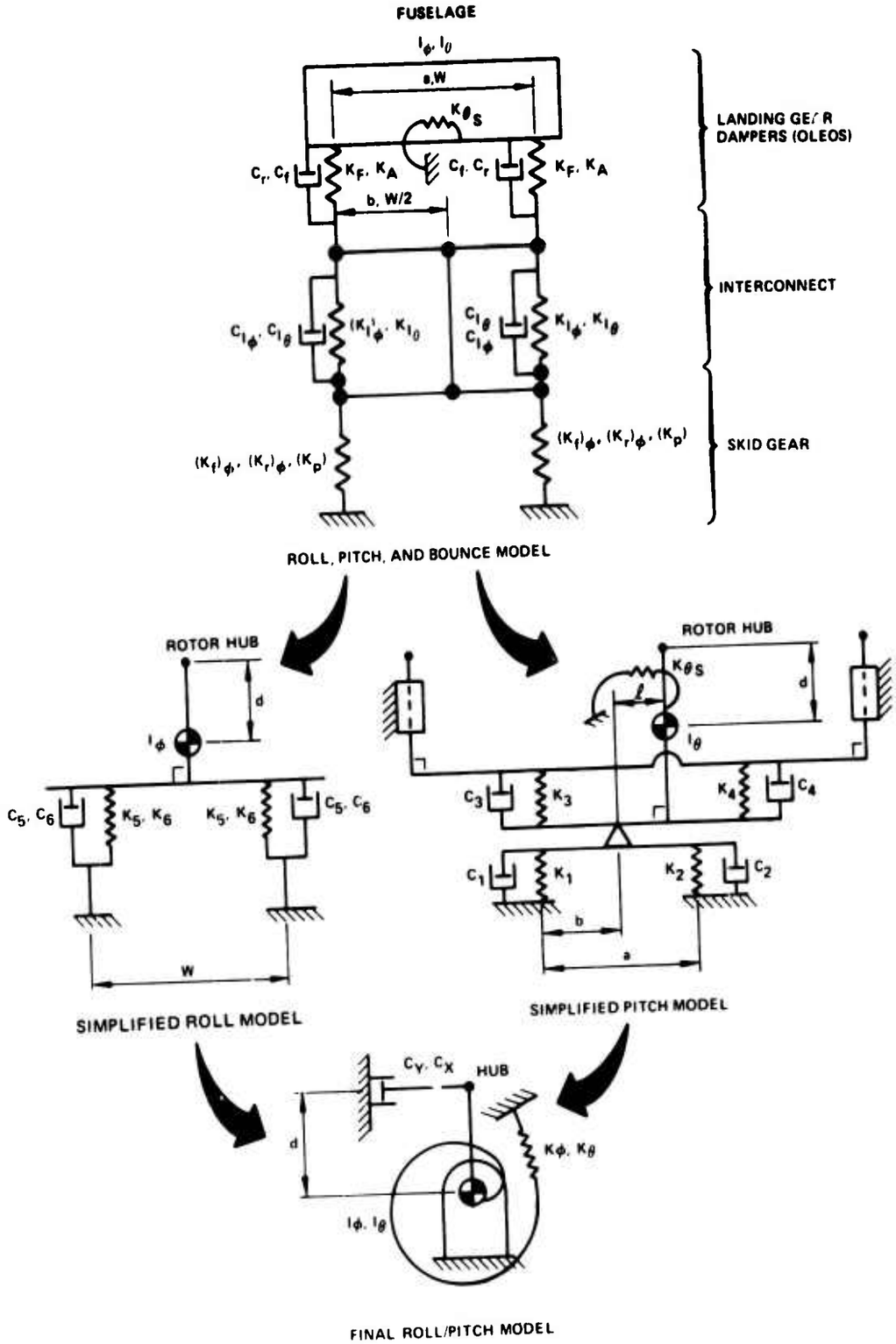

Figure C-1. Reduction of Basic Roll, Pitch, and Bounce Model

TABLE C-1. GROUND RESONANCE ANALYTICAL MODEL ELEMENTS

Identification	Min Fly Wt 1345 lb	Maximum GW 2800 lb			Design GW 2550	Description
	Interconnected 92131	Interconnected 92131 Damper	Failed Interconnected 92131 Damper	Failed Interconnected 6340 Damper	Basic OH-6A 6340 Damper	
Lengths, in.						
a	53.66	53.66	53.66	53.66	53.66	Distance between crosstubes at ground contact, (pitch)
W	90.32	90.32	90.32	90.32	76.00	Distance between skid tubes (roll)
ℓ	9.0	6.18	6.18	6.18	-	Moment arm of center of gravity about geometrical pitch center
d	43.64	51.3	51.3	51.3	50.72	Vertical distance from rotor to center of gravity
b	28.38	28.38		-	-	Distance from front crosstube to geometric pitch center
Stiffness lb/in.						
K_f	38.	208	186	344	273	Front oleo stiffness ratioed to ground contact point
K_A	47.	307	341	1075	964	Aft oleo stiffness ratioed to ground contact point
$(K_I)_\phi$	36.78	36.78	"	"	"	Roll interconnection stiffness converted to ground contact = $2\,(K_\phi)_I/W^2$
$(K_I)_\theta$	10 .2	104.2		"	"	Pitch interconnection stiffness converted to ground contact = $2\,(K_\theta)_I/a^2$
$(K_f)_\phi$	300	300	300	300	385	Front crosstube vertical stiffness for bounce and roll
$(K_r)_\phi$	500	500	500	500	731	Aft cross tube vertical stiffness for bounce and roll
K_p	785	785	785	785	1394	Skid gear pitch stiffness with rigid oleos converted to ground contact point.
K_1	33.7	122.8	-	-	-	Equivalent bounce stiffness per side front
K_2	43.	190.2	-	-	-	Equivalent bounce stiffness per side at aft
K_3	26.9	63.8	150	239	-	Equivalent interconnection stiffness per side front
K_4	31.1	70.8	237	454	-	Equivalent pitch interconnection stiffness per side rear
K_5	17.6	28.83	115.	160	159	Equivalent roll stiffness per side, front
K_6	19.9	31.45	203	341	416	Equivalent roll stiffness per side, aft

TABLE C-1 - Continued

Identification	Min Flg Wt 1345 lb	Maximum GW 2800 lb			Design GW 2550	Description
	Interconnected 92131	Interconnected 92131 Damper	Failed Interconnected 92131 Damper	Failed Interconnected 6340 Damper	Basic OH-6A 6340 Damper	
Stiffness $\frac{\text{lb/in.}}{\text{rad}}$						
K_{θ_s}	214,000	214,000	214,000	214,000	282,000	Pitch stiffness of oleoless skid gear per side
$(K_\theta)_I$	150,000	150,000	"	"	"	Interconnection stiffness per side (pitch)
K_θ	512,000	621,000	985,000	1,425,000	-	Total pitch stiffness
K_{Φ_I}	150,000	150,000	"	"	"	Roll interconnection stiffness for each opposing cross tube set
K_Φ	153,000	245,900	1,297,000	2,044,000	1,602,000	Total roll stiffness
Damping lb/in./sec						
C_f	8.36	8.36	8.36	4.66	6.28	Front oleo damping converted to ground contact point
C_r	10.54	10.54	10.54	5.88	8.43	Rear oleo damping converted to ground contact point
$(C_I)_\Phi$	3.68	3.68	-	-	-	Interconnection system roll damping converted to ground contact point = $\frac{2\,(C_\Phi)_I}{W^2}$,
$(C_I)_\theta$	10.42	10.42	-			Interconnection system pitch damping converted to ground contact point = $\frac{2\,(C_f)_I}{a^2}$
C_1	6.36	2.87	-	-	-	Front Bounce
C_2	8.62	4.01	-	-	-	Rear Bounce
C_3	3.57	4.43	5.42	2.25	-	Front Pitch (Equivalent Ground Contact Point Damping)
C_4	4.13	5.15	5.08	1.046	-	Rear Pitch (Equivalent Ground Contact Point Damping)
C_5	1.68	2.26	2.89	.982	2.06	Front Roll (Equivalent Ground Contact Point Damping)
C_6	1.83	2.66	3.53	.888	1.86	Rear Roll (Equivalent Ground Contact Point Damping)
C_x	6.81	5.6	5.74	1.79	-	Final equivalent hub pitch damping
C_y	7.52	5.84	9.98	.770	4.20	Final equivalent hub roll damping

TABLE C-1 - Continued

Identification	Min Fly Wt 1345 lb	Maximum GW 2800 lb			Design GW 2550	Description
	Interconnected 92131	Interconnected 92131 Damper	Failed Interconnected 92131 Damper	Failed Interconnected 6340 Damper	Basic OH-6A 6340 Damper	
Damping in. /lb rad/sec						
$(C_\phi)_I$	15,000	15,000	0	0	0	Interconnection roll damping for opposing crosstube set
$(C_\theta)_I$	15,000	15,000	0	0	0	Interconnection pitch damping per side
Moment of Inertia lb/in. sec^2						
I_ϕ	2251	3697	3697	3697	3569	Roll moment of inertia
I_θ	9090	10,885	10,885	10,885	-	Pitch moment of inertia
Natural Frequencies radians/sec						
W_ϕ	8.28	8.00	18.7	23.51	21.58	
W_θ	7.59	7.77	9.51	9.57	-	

MASS AND MOMENT-OF-INERTIA PROPERTIES

The moment of inertia of the fuselage about the center of gravity was calculated from the data in Reference 6, corrected to the principal axis, and reduced by the active weight of two of the four blades. The active weight of one blade is given by

$$We = \frac{\sigma_\zeta^2}{I_\zeta}$$

where We = active weight of one blade = 17.1 lb

I_ζ = Lag hinge inertia of one blade = 176,200 lb-in.^{2}

σ_ζ = Moment about lag hinge = 1735 in.-lb

---

[6] Conlin, J. F., CALCULATED MASS PROPERTY DATA, HUGHES HELICOPTER MODEL 369A, Hughes Tool Company - Aircraft Division Report 369-W-8003, April 1966.

For a noninterconnected system, the maximum gross weight of 2800 pounds is most critical for ground resonance. The oleo stiffness is proportional to the square of the oleo load whereas roll inertia is increased at a rate less than the gross weight. However, for the interconnected system, the roll stiffness is relatively constant, and therefore the minimum inertia associated with the minimum flying weight, 1394 pounds, is likely to be most critical for ground resonance.

STIFFNESS DATA

Skid Gear

The skid gear contributes significantly to the pitch stiffness for the interconnected and noninterconnected systems due to torsion and bending of the skid tubes and the cross tube. The values used were determined from a computerized model of the skid gear without oleos.[7]

The bending of the cross tubes and the deflection of the fuselage attach points are in series with the roll interconnection, the oleo spring, and the damping, which reduces the effective roll damping and stiffness for both the interconnected and noninterconnected systems. The values used were determined as above with rigid links replacing oleos.

Oleo Stiffness

The oleo stiffness was determined using the air spring formula ($K_o = \frac{kA^2P}{V}$), Boyle's law ($PV = C$) and the fact that the volume of air in equilibrium solution with the oil is equivalent to 10 percent of the oil volume at the prevailing pressure where

K_o = Oleo stiffness, lb-in.

k = Compression exponent, 1.4 for adiabatic compression

A = Piston area = 1.35 $in.^2$

P = Absolute pressure, Psi

V = Volume, $in.^3$

---

[7] Soltis, S., STRESS ANALYSIS FUSELAGE 369-S-3004, unpublished.

This yields

$$K_s = \frac{kF_s^2}{F_o(\ell_o + \Delta\ell) - F_s R\Delta\ell}$$

where

$K_s = \frac{K_o}{R^2}$ = oleo stiffness reduced to the skid location, lb-in.

F_s = load at skid = $\frac{\text{oleo load}}{R}$, lb absolute

F_o = Equilibrium oleo load (PA) fully extended, lb absolute

ℓ_o = Gas volume/piston area at fully extended position, in.

$\Delta\ell$ = .10 (Oil Volume)/A, in.

R = Ratio of skid vertical deflection to oleo vertical deflection (rigid body motion)

Table C-2 shows the values of the parameters used in determining the oleo stiffness for the oleos and loads used. (F_s was determined by approximating the pitch stiffness with an average oleo stiffness, determing the moment about the geometric pitch center of the skid gear with an assumed skid angle and iterating till the assumed angle matched the calculated angle. The differential load between front and rear oleos was used to determine F_s front and F_s rear.)

DAMPING

Oleo Damping

Oleo damping was based on the results of oleo bench tests shown in Reference 8. A conservative equivalent viscous damping at the maximum velocity tested, 12.56 in./sec, was determined by the force/velocity ratio and reduced to skid location by

$$C_s = \frac{Fe}{V}\frac{1}{R^2}$$

[8] Neff, J. R., GROUND RESONANCE SUBSTANTIATION, MODEL 369H SERIES, Hughes Tool Company - Aircraft Division Report 369-V-8006.

TABLE C-2. OLEO PARAMETERS								
Condition	F_s Front	F_s Rear	R Front	R Rear	F_o lb	ℓ_o	$\Delta\ell$	Oleo Damping lb/in./sec
2800 Max GW interconnected 369H92131 oleos	648	768	3.2	2.85	953	4.17	1.01	85.6
2800 GW non interconnected 369H92131 oleos	619	795	3.2	2.85	953	4.17	1.01	85.6
1354 Min FW interconnected 92131 oleos	326	364	3.2	2.85	953	4.17	1.01	85.6
2800 Max GW nonintercon-nected 369H6340	585	829	3.2	2.85	685	3.78	1.01	47.75
2550 DGW Aft CG 369A3640 oleos Std gear	511	779	2.75	2.38	575	3.78	1.01	47.75

where

C_s = Oleo damping reduced to skid loaction, $\frac{\text{lb}}{\text{in./sec}}$

Fe = Equivalert viscous damping oleo force, lb

V = Velocity corresponding to Fe, in./sec

R = Ratio of oleo deflection to skid vertical deflection

Tables C-1 and C-2 show the values used for the 369H6340 and the 369H92131 oleos. The 369H6340 oleo has the same dynamic characteristics as the 369A6350 oleo.

Blade Damping

The multistage friction damper used on the OH-6 has damping that is amplitude sensitive. The damping force is considered to be insensitive to frequency. The equivalent viscous damping is given by

$$(C_\zeta)_e = \frac{E_o}{\pi(\zeta_o)^2 \omega} \quad \text{Equivalent blade damping, } \frac{\text{in.-lb}}{\text{rad/sec}}$$

See Reference 7 for derivation.

The value used for $\frac{E_o}{\pi(\zeta_o)^2}$ in this analysis is $5.5\ (10)^4$ in.-lb., the lowest value for the 369A1400-601 damper shown in Figure III-6 of Reference 7.

Damping Product Ratio Analysis

Table 2 shows the damping product ratio for the interconnected and non-interconnected systems analyzed. (Damping product ratio = [damping product available/damping product required])

From Reference 7 for the isotropic case

$$\frac{\text{damping product available}}{\text{damping product required}} = \frac{g^2}{N\sigma_\zeta^2} \left(\frac{E_o}{\pi \zeta_o^2}\right) \frac{C}{(\omega^3)}$$

where

g = acceleration of gravity, 386 $\frac{\text{in.}}{\text{sec}^2}$

σ_ζ^2 = Blade lag hinge moment, 1735 in.-lb

N = Number of blades, 4

[7] Soltis, S., STRESS ANALYSIS FUSELAGE 369-S-3004, unpublished.

C = Equivalent hub damping $\frac{\text{lb}}{\text{in./sec}}$

$\frac{E_o}{\pi \zeta_o^2}$ = Blade damping parameter, = 55,000 lb-in.

ω = Hub natural frequency, rad/sec $= \sqrt{\frac{K_\phi}{I_\phi}}$ or $\sqrt{\frac{K_\theta}{I_\theta}}$

The hub natural frequency, ω, was calculated from the roll inertia and from the series combination of the oleo stiffness, the crosstube bending stiffness (roll) or the rigid oleo skid gear pitch stiffness, and the interconnection system stiffness (where appropriate). The appropriate oleoless skid gear pitch stiffness was added to this series combination for pitch natural frequency determinations. (See Figure C-1.)

The hub damping, C_x or C_y, was calculated using the following equivalent damping relationship for a spring and damper in series with a spring (Reference 9)

$$C_{eq} = C \frac{K_s^2}{(K_s + K_c)^2 + C^2 \omega^2} = C \left(\frac{K_{eq}}{K_s}\right)^2 \frac{1}{\left(1 + \frac{C^2 \omega^2}{(K_s + K_c)^2}\right)}$$

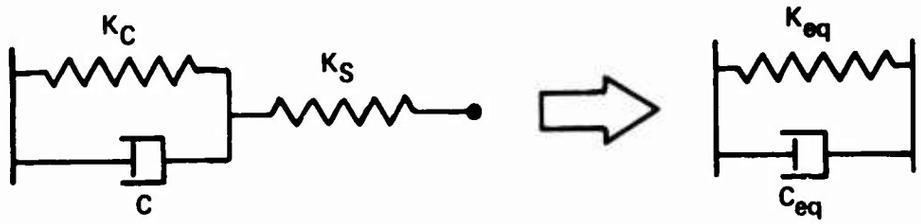

where

C_{eq} = Equivalent damping $\frac{\text{lb}}{\text{in./sec}}$

C = Uncorrected damping $\frac{\text{lb}}{\text{in./sec}}$

---

[9] Mil, M. L., et al, HELICOPTER CALCULATION AND DESIGN, VOLUME II VIBRATIONS AND DYNAMIC STABILITY, NASA TTE-519, May 1968.

K_c = Stiffness in parallel with uncorrected damping, $\frac{lb}{in.}$

K_s = Stiffness in series with uncorrected damping, $\frac{lb}{in.}$

K_{eq} = Equivalent stiffness = $\left[\frac{1}{K_c} + \frac{1}{K_s}\right]^{-1}$, $\frac{lb}{in.}$

For the case where the interconnect spring, K_I, and the damper, C_I, were in series with the oleo spring, K_O, and the damper, C_O, corrected to the skid tube/crosstube intersection, and a skid gear stiffness, K_s, an

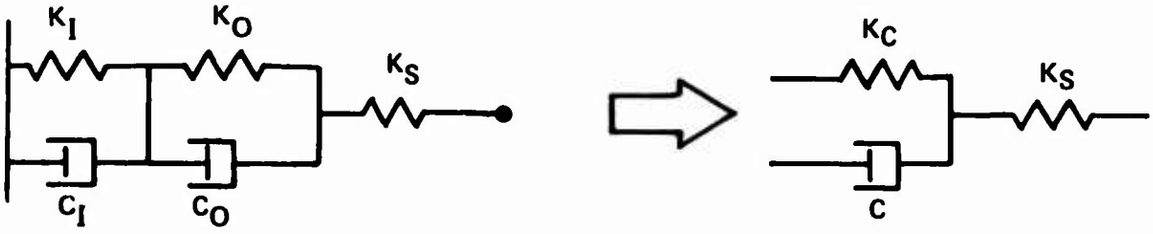

equivalent spring and damper were conservatively determined by summing the equivalent damping determined for the damped springs alone while assuming the other damped spring to be undamped. The damping thus determined was then corrected for the skid gear stiffness. The damping levels used for this analysis had very little effect on the equivalent stiffness and were neglected.

After the determination of the equivalent damping at skid tube/crosstube intersections, the hub damping was determined by assuming that roll or pitch takes place about the principal axis, which is the same condition as in Reference 8. Then hub damping, C_x and C_y, are given by

[8] Neff, J. R., GROUND RESONANCE SUBSTANTIATION, MODEL 369H SERIES, Hughes Tool Company - Aircraft Division Report 369-V-8006.

$$C_x = \frac{(C_3 + C_4)\, 2\left(\frac{a}{2}\right)^2 + (C_1 + C_2)\, \ell^2}{d^2}$$

$$C_y = \frac{(C_5 + C_6)\, 2\left(\frac{W}{2}\right)^2}{d^2}$$

where

$C_1, \ldots\ldots C_6$ are the appropriate equivalent dampings as given and defined in Table C-1 and shown in Figure C-1; W, ℓ, d are the distances given and defined in Table C-1 and shown in Figure C-1.

SYMBOLS

A_1	Horizontal distance from gear pivot point to skid (see Figure A-1) - in.
A_2	Vertical distance from gear pivot to skid (see Figure A-1) - in.
A_3	Perpendicular distance from gear pivot point to oleo (see Figure A-1) - in.
C_F	Ground friction factor - nondimensional
C_{oleo}	Ratio of oleo stroke to gear deflection at ground, assuming the cross tube is infinitely rigid - nondimensional
C_2	Oleo damping constant (see equation 10) - lb $sec^2/in.^2$
CG	Center of Gravity
Exp	Exponent in oleo spring force equation
F_c	Force in oleo damper, $F_c = C_2 (\dot{X}_{oleo})^2$ - lb
F_{Gnd}	Force on ground - lb
F_{oleo}	Total force in oleo - lb
F_s	Force in oleo spring, $F_s = \frac{K_{oleo}}{\left(1 - \frac{X_{oleo}}{S_{oleo}}\right)}$ Exp - lb
F_x	Force in the cross tube
H_F	Vertical distance from front skid to CG - in.
H_R	Vertical distance from rear skid to CG - in.

I	Total ship pitch moment of inertia - lb-in.-sec^2
K_{air}	Spring constant in oleo due to air entrapped in the oil - lb/in.
K_c	Spring constant of skid tube - lb/in.
K_{oleo}	Constant in oleo spring (see equation 10) - lb
K_x	Spring constant of cross tube - lb/in.
L	Rotor lift - lb
m	Helicopter mass - lb-sec^2/in.
S_{oleo}	Constant in oleo spring (see equation 10) - in.
W	Helicopter weight - lb
X_{CG}	Relative vertical deflection of the CG - in.
X_{oleo}	Oleo stroke - in.
X_{GR}	Vertical deflection of skid due to oleo compression - in.
X_1	Vertical deflection of cross tube due to bending - in.
X_2	Relative vertical deflection of pivot point - in.
X'_{2_f}	Vertical distance of front pivot point above rear pivot point during nose high landing (see Figure A-2) - in.
Y_f	Horizontal distance from front skid to CG - in.
Y_R	Horizontal distance from rear skid to CG - in.
α_i	Initial pitch attitude at touchdown - rad
θ	Pitch angle - rad

ΔV_Z	Downward drop velocity at touchdown - ft/sec
Ψ_i	Initial roll attitude at touchdown - deg

Subscripts

f	Refers to front cross tube
R	Refers to aft cross tube

Superscripts

$\cdot$	First derivative
$\cdot\cdot$	Second derivative